Odden ice melt linked to Labrador Sea ice expansions and the Great Salinity Anomalies of 1970-1995

David Allan (The Dell, St Albans, UK) and Richard P Allan (Department of Meteorology and National Centre for Earth Observation, University of Reading, UK)

Abstract

In each of the last three decades of the 20th century there were unprecedented expansions of sea-ice over the Labrador Sea basin and influxes of cold fresh water into the subpolar gyre which have been described as the Great Salinity Anomalies (GSAs). Employing data for sea surface temperature, salinity and sea ice cover, we propose that these events were downstream consequences of the expansion and subsequent melting of so-called 'Odden' ice formed over the deep basin of the Greenland-Iceland-Norway (GIN) Sea in the 1960s, 1970s and1980s and additional to the normal East Greenland shelf sea-ice. We expand previous findings that Odden ice expansions were linked to winter episodes of high atmospheric pressure north of Greenland that directed freezing Arctic winds across the GIN Sea and may also have been associated with increased Arctic sea-ice volume leading to enhanced ice export through Fram Strait. We show that cold water and ice derived from Odden melting in the summer passed through Denmark Strait and along the East Greenland shelf, and accumulated in the Labrador Sea, creating favourable conditions for winter ice formation during particularly cold years in southwest Greenland. Meltwater from Odden and Labrador Sea ice appeared to break out into the subpolar gyre in the fall of 1982 and 1984 respectively and this cold water represents the likely source of the 1982-1985 GSA. These findings further our understanding of the physical processes linking ice formation and melt with ocean circulation in this key component of the climate system.

Plain Language Summary

Global warming has its largest effects in the Arctic where enhanced melting of sea-ice will send increased cold meltwater southwards into the North Atlantic with possible effects on climate in Europe and North America. Here we describe an intermediate source of Atlantic cold fresh water derived from melting of the Odden ice, a variable body of new sea-ice which appeared in the far north Atlantic basin in three periods during the 1960s, 1970s and 1980s. Odden ice formed over deep water in response to freezing winter winds together with enhanced transport of ice from the Arctic Sea and was additional to the normal East Greenland sea-ice near the coast. Three subsequent periods of Odden melting in summer released large pulses of cold fresh water and ice which entered the Labrador Sea basin 2000 km away and facilitated three corresponding periods of unprecedented sea-ice formation in the following winter. We identify Odden and Labrador Sea meltwater as the sources of the three Great Salinity Anomalies that spread cold low-salt water around the northwest Atlantic in the 1970s, 1980s and 1990s and may have affected North Atlantic climate.

Key words:
Labrador Sea ice; Odden ice feature; Great Salinity Anomalies

Key points

1 Three late 20th century expansions of Odden ice in the far North Atlantic constituted a subsidiary reservoir of Arctic fresh water.

2 Three releases of fresh water from the Odden are linked to three episodes of unprecedented Labrador Sea ice cover between 1970 and 1995.

3 Meltwater from Odden and Labrador Sea ice represents the likely precursor of the three Great Salinity Anomalies.

Figure 1. Map of the northern North Atlantic region including Greenland, Iceland and Newfoundland

BB is Baffin Bay, DS is Davis Strait, LS is the Labrador Sea, SPG is the Subpolar Gyre formed between the shelf Labrador Current moving south (LC, light blue), the North Atlantic Current moving northeast (NAC, red) and the East and West Greenland currents. GIN is the Greenland-Iceland-Norwegian Sea, FS is Fram Strait, S is Svalbard, CF is Cape Farewell, FC is Flemish Cap, TGB is the Tail of the Grand Banks, Ilu is Ilussac, Q is Qaqortoq, Itt is Ittoqqorqoormiit. The North Atlantic Current (NAC) is traced from the TGB, to the east of FC, around Northwest Corner, (NWC) and as far as the Charlie-Gibbs Fracture Zone (CGFZ) visible at 53°N. Two land areas of Greenland are marked and referred to in the text; one is in the southwest (SW) and the other in the east (E). This map is based on the publicly available Google Earth Pro and the paths of the major currents are derived from the schemes proposed by Rossby (1996), Fratantoni and McCartney (2009) and Stendardo et al. (2020).

Introduction

Each winter, sea-ice extends southwards from the Labrador Sea and along the Labrador shelf sometimes as far as Flemish Cap (47°N 45°W) and the Tail of the Grand Banks (43°N 50°W) but also down the eastern Greenland shelf, usually as far as Cape Farewell (60°N 44°W) (Deser et al. 2002). Although some of this sea ice may be produced locally by cold winds blowing off the Labrador and Greenland land masses, both seasonal ice expansions are driven by considerable transport of Arctic ice southwards through (respectively) Davis Strait and Fram Strait but mainly confined to the continental shelf regions (Aagaard and Carmack 1989; Mysak and Manak 1989). This ice together with its burden of icebergs gradually melts *en route* and eventually contributes cold fresh water to the Labrador Sea and the North Atlantic.

A potential third source of North Atlantic sea-ice and cold fresh water was described by Schuchman et al. (1998) as the Odden ice feature. This was additional to the normal East Greenland shelf sea-ice and expanded in three periods between 1960 and 1990 in the deep central basin of the Greenland-Iceland-Norway (GIN) Sea (the area bounded by Greenland, Iceland, Norway and 80°N; see Figure 1).

Following Schuchman et al. (1998) we will refer to the Odden ice feature simply as the Odden and note that it does not have a precise location because it is so variable in extent and position. Prior to 2000, the Odden appeared from December to March as an eastward expansion of the East Greenland sea-ice but was different in character and much more variable from year to year and even from day to day compared with the coastal ice (Shuchman et al. 1998; Rogers and Hung, 1998). Unlike the latter, which was largely confined to the shallow shelf regions, the Odden expanded across the deepest waters (>3000m) of the GIN Sea north of Jan Mayen Island (71°N 8°W) where it was frequently exposed to some of the fiercest storms in the northern hemisphere. It sometimes extended further than $3x10^5$ km^2 beyond the mean East Greenland sea-ice margin but was liable to rapid changes in area and thickness which are likely to have involved a number of cycles of freezing and thawing within a single year (Shuchman et al. 1998; Comiso et al. 2001). This lability of Odden ice reflects the observation that it was largely recently-formed pancake-frazil ice, consistent with its turbulent environment and contrasting with the more coherent multi-year ice exported from the Arctic. (Wadhams and Comiso 1999; Wadhams and Wilkinson 1999; Niederdrenk and Mikolajewicz 2016). This unstable ice permits continued high heat loss from the ocean and fast ice growth, in contrast to the blanketing effect of the more coherent shelf pack-ice (Wadhams and Comiso 1999). In some years (particularly 1987 and 1996) there was a component of older, thicker ice in the Odden and this may represent ice **advected** from the Arctic through Fram Strait and essentially different from the characteristic **thermodynamic** ice formed *in situ* under extreme winter conditions (Wadhams and Comiso 1999). The advected ice could be carried eastwards in the Jan Mayen Current, a branch of the East Greenland Current which passes north of Jan Mayen Island (Bourke et al. 1992).

The Odden has long been known and identified by mariners but markedly increased in area during the mid-1960s, early 1980s and late 1980s although it was more rarely observed thereafter (Visbeck et al. 1995; Shuchman et al. 1998; Rogers and Hung, 1998; Germe et al. 2011; Selyuzhenok et al. 2020). Its appearance in the second half of the 20th century was initially attributed to periods of unusually cold westerly winds in

winter, sweeping from the Greenland ice-cap across the region north of Jan Mayen Island (71°N 8°W) and west of Svalbard (79°N 18°E) (Shuchman et al. 1998).

Later work has favoured the idea that increased transport of Arctic ice through Fram Strait is the stimulus for sea ice formation in the GIN Sea. Using 'an optimized dynamic/thermodynamic sea ice model' maintained by National Center of Environmental Prediction/ National Center of Atmospheric Research, Hilmer et al. (1998) conducted simulations linking changes in transport of ice through Fram Strait to a distribution of sea-ice in the GIN Sea closely resembling the Odden, with ice as much as 4m thick in places. Köberle and Gerdes (2003) carried out simulations using a coupled ocean–sea ice model (Geophysical Fluid Dynamics Laboratory Princeton University, Princeton, NJ modular ocean model (MOM-2) that demonstrated peaks of ice export through Fram Strait in 1968, 1980 and 1989 (similar to those seen by Smedsrud et al. 2017) which were related to peaks of Arctic ice volume in 1966, 1980 and 1988 (similar to Schweiger et al. 2019). These findings suggest that an important factor in increasing ice export and expanded Odden sea-ice cover (SIC) may be a prior increase in Arctic sea-ice volume.

Several studies have also suggested that unusually high sea level pressure (SLP) north of Greenland would generate northerly winds promoting export of ice through Fram Strait and consequent increased sea ice cover (SIC) in the GIN Sea (Mysak and Manak 1989; Hilmer et al. 1998; Rogers and Huang 2008; Germe et al. 2011). Tsukernik et al. (2010) pointed out the relationship between increased motion of ice through Fram Strait and a SLP dipole formed between high pressure over Greenland and low pressure over the Barents Sea. Strong northerly winds generated by this dipole in winter are very likely to have increased Odden ice directly by strong surface cooling but also would have increased ice transport through Fram Strait, probably contributing to the Odden. It is plausible that many of the factors which are associated with Odden development including increased ice volume in the Arctic, high pressure north of Greenland, increased northerly winds bringing more ice through Fram Strait and cold air descending from the Greenland ice cap could all be aspects of the negative phase of the Arctic Oscillation (Overland and Wang 2005).

The Odden is of particular interest because its extent defines the area of open water remaining to the north (the Nordbukta) which is one of the few major sites of deep convection in the Northern Hemisphere (Visbeck et al. 1995). In some years and some months when the Nordbukta is ice-free the Odden appears as a tongue of ice projecting northeastwards away from Greenland whereas in other years when the Nordbukta is frozen, the Odden presents as an easterly bulge on the sea-ice front (Wadhams and Comiso 1999; Comiso et al. 2001). Because sea-ice and cold fresh meltwater derived from it are likely to inhibit deep convection, the formation and dissolution of the Odden could potentially exert an important influence on deep convection in the Nordbukta and it has been suggested that the great reduction in the Odden area since 2000 might have increased deep convection in the Nordbukta (Selyuzhenok et al. 2020). Conversely, Labrador Sea ice expansion in 1972 may have terminated the period of deep convection in the Labrador Sea which was described by Lazier (1980). Thus, in the GIN sea and the Labrador Sea, two regions far distant from one another, high SIC may limit deep convection.

Close et al. (2018) studied the factors which influence the extent of sea-ice cover in the Labrador Sea and concluded that unusually large amounts of cold fresh water exported from the Irminger Sea led to surface stratification in the Labrador Sea and this facilitated freezing on 3-4 occasions between 1970 and 1995. They identified two regions of ice (R1 and R2) in the southern Labrador Sea which expanded around 1972-74, 1983-84 and 1990-95 in response to increased influx of fresh water from East Greenland perhaps in conjunction with unusually strong cold north-westerly winds in winter. This input was assessed as an average of 150 km^3 with a maximum of 460 km^3/year which is comparable to the estimate of Schmidt and Send (2007) of about 620 km^3 for the maximum volume of fresh water carried into the West Greenland Current from East Greenland in June – August from 1996-2001. Deser et al. (2002) noted previous findings (Mysak and Manak 1989) that periods of ice expansions in the Labrador Sea were preceded by much earlier ice expansions in the GIN Sea east of Greenland. Here we present evidence that the Odden is the most credible source of three tranches of fresh water which not only promoted three episodes of freezing in the Labrador Sea but may also have represented the origin of the three Great Salinity Anomalies (GSAs) of the late 20th century.

These GSAs were large tranches of colder and fresher water introduced into the Labrador Sea from the Irminger/Greenland Sea, which were propagated around the North Atlantic subpolar gyre (SPG) in each of the three decades beginning in 1970 and believed to derive originally from Arctic ice exported through Fram Strait (Dixon et al. 1988; Aagaard and Camack 1989; Mysak and Manak 1989; Belkin et al. 1998; Belkin 2004; Häkkinen, 1993, Köberle and Gerdes 1993; Haak et al. 2003; Curry and Mauritzen 2005). As summarised by Belkin et al. (1998) and Belkin (2004), the cold fresh water of the GSAs was introduced from the Irminger Sea and followed the East Greenland Current around Cape Farewell into the West Greenland current as far as Fylla Bank (63^{o}N 54^{o}W). The GSA water then entered the SPG, initially following the Labrador Current, a large part of which is retroflected and entrained into the North Atlantic Current (NAC) close to the Tail of the Grand Banks (Krauss et al. 1986; Fratantoni and McCartney; 2010). The GSA continued to follow the northern branch of the NAC east of Flemish Cap (Rossby 1996) and through the reticulations of the Mid-Atlantic Ridge (Bower and von Appen 2008; Stendardo et al. 2020) including the Charlie-Gibbs Fracture Zone (CGFZ), Faraday and Maxwell Fracture Zones (Bower and von Appen, 2008) before dissipating southwards or recycling south of Iceland. It is worth emphasising that as originally described (Ellet and Blindheim, 1992; Belkin et al. 1998 based on the schemes of Krauss et al. 1986 and Dixon et al. 1988), the GSA first occupied the descending (western) limb of the SPG (the Labrador Current as far as the TGB) and then merged with the ascending limb of the SPG (the NAC) from the TGB to the east of Flemish Cap and through the CGFZ (see Figure 1). The beginnings of the three GSA periods at Fylla Bank were in 1971, 1982, (1990/1993) (Belkin 2004, his Figure 2), **before** the corresponding ice maxima in the Labrador Sea (1972, 1983-4 and 1990-1993) (Deser et al. 2002) and consistent with the hypothesis of Close et al. (2018) that cold fresh surface waters introduced from the Irminger Sea induced stratification in late summer which promoted sea-ice formation in the Labrador Sea in the following winter.

This investigation attempts to define how the three major expansions of sea-ice in the Labrador Sea basin in the last decades of the 20th century (Deser et al. 2002) could be related to changes in ice cover over the deep GIN Sea (the Odden) and eventually to increases in Arctic ice area and transport through Fram Strait. Our work suggests that an important intermediary in the chain between the Arctic and the Labrador Sea was the formation and dissolution of Odden ice which sent large amounts of ice and fresh water southwards along the East Greenland shelf, promoting three major freezing episodes over the deep basin of the Labrador Sea during particularly cold periods in SW Greenland. We suggest that melting of Odden ice together with the subsequent melting of the Labrador Sea ice are the source of the episodes of cold fresh water release into the subpolar gyre (SPG) which became known as the Great Salinity Anomalies (Belkin et al. 1998).

Data and Methods

Sea surface temperature (SST) and sea ice cover (SIC) data (1^{o} latitude/longitude resolution) were obtained from the Hadley Centre Sea Ice and Sea Surface Temperature dataset (HadISST; v2.2 was available for sea ice but v1.1 was the latest version available for SST) (Rayner et al. 2003; Titchner and Rayner 2014). These combine in situ observations with statistical interpolation techniques to provide a global ocean coverage at 1^{o} latitude/longitude resolution since 1870; data since 1960 over the North Atlantic are considered here. Optimum Interpolation Sea Surface Temperature (OISST) V2 data (Huang et al. 2021) provide a higher resolution (0.25^{o} latitude/longitude) daily estimate of ocean surface temperature since September 1981. This dataset applies multiple satellite and *in situ* estimates which can introduce artificial changes as the observing system changes over time, so here the version using Advanced Very High Resolution Radiometer (AVHRR) infrared satellite measurements only are employed. The infrared satellite measurements are valid for cloud-free conditions and can be further contaminated by cloud or aerosol. They are sensitive to diurnal heating of the surface skin layer so can contain biases relative to *in situ* estimates though this is mitigated through a calibration procedure (Huang et al. 2021). The benefits of high resolution estimates from an independent, homogeneous source are deemed beneficial and complementary to the lower resolution HadISST observations. A consistent long term blended climatology 1971-2000 is used in this case in the construction of daily anomalies. A quality controlled sub-surface ocean temperature and salinity dataset (EN4.2.2; Good et al. 2013) is used to sample 0-400m salinity (S400) and ocean heat content (OHC400). These products apply objective analysis using persistence-based forecast of the ocean state from the previous month to a quality-controlled set of vertical profiles of temperature and salinity to generate 1^{o} latitude/longitude gridded estimates.

Air temperature data from Greenland coastal sites were obtained from Cappelen (2020). Air temperatures in Svalbard (78^{o}-79^{o}N 14^{o}-16^{o}W) were obtained from the GISS Surface Temperature Analysis (GISTEMP), version 4 (Lenssen et al. 2019). Air temperature data from the Climatic Research Unit (CRU TS v4.04) for areas of SW and E. Greenland are described by Harris et al. (2020). Arctic Oscillation Index (AOI) data, constructed by the National Centre for Environmental Prediction/Climate Prediction Center (NCEP/CPC; see Open Data) from daily 1000 hPa height anomalies poleward of 20°N that are projected onto a leading mode of northern hemisphere high latitude atmospheric variability, are used here to characterise the strong and weak westerly wind phases affecting the north Atlantic and Greenland.

Sea level pressure (SLP) and surface heat flux data on a 0.25^{o}x 0.25^{o} grid were obtained from the European Centre for Medium-range Weather Forecasts 5th generation reanalysis (ERA5; Hersbach et al. 2020). This combines multiple observing systems with a high-resolution atmosphere model using four-dimensional-variational data assimilation. ERA5 Surface heat fluxes were computed from the surface latent and sensible heat fluxes, the net surface shortwave radiation and the net surface longwave radiation. SLP measurements are assimilated as part of the ERA5 reanalysis system, and so are closely constrained by observations, this is not the case for surface fluxes which are calculated based on the surface and atmospheric conditions using detailed parametrization of turbulent and radiative fluxes. The accuracy of these products is therefore dependent on the representation of surface and near surface temperature, humidity and wind fields and also the atmospheric meteorological profiles aloft, including cloud cover and properties. Net surface downward flux is computed as the sum of surface downward latent, sensible, net shortwave radiation and net longwave radiation fluxes, all integrated over each month to convert from Wm^{-2} to GJ/m^{2}. For all datasets, deseasonalised anomalies were calculated relative to a monthly climatology over a base period as stated. Spatial re-gridding was performed using bi-linear interpolation. Pearsons correlation and linear least squares fit (minimising chi squared error) were applied to determine trends and goodness to fit. Two or three dimensional data were processed and plotted using IDL Graphics, NV5 Geospatial nv5geospatial.com.

Results

1. Three expansions of sea ice in the Labrador Sea were predated by three expansions and dissolutions of the Odden Ice in the Greenland-Iceland-Norway (GIN) Sea

Previous work on the three major ice expansions in the Labrador Sea had been restricted to the Labrador Sea and inputs to it of ice and fresh water from Baffin Bay and the Irminger Sea (Deser et al. 2002; Close et al. 2018). In contrast, we have examined how the three Labrador Sea ice expansions between 1970 and 1995 might be related to sea-ice changes which are known to have occurred in the GIN Sea in the far north of the Atlantic Ocean. Figure 2 compares the sea-ice fraction **anomalies** in the GIN Sea with those in the Labrador Sea between 1960 and 1995. In February 1960 the GIN Sea had considerably less ice than normal (red tints) except for a pronounced positive anomaly (blue tints) near Svalbard (80^{o}N). Positive anomalies increased overall throughout the 1960s and by 1969 they extended from Svalbard to Iceland occupying about $4x10^{5}$ km^{2}. The region showing these large positive anomalies corresponded well with previous descriptions of the Odden ice feature (outlined in the Introduction) which is manifested as a variable area of ice in the GIN Sea east of and additional to the normal sea-ice occupying the East Greenland shelf region.

In contrast to this expansion of the Odden, which by February 1969 enveloped Jan Mayen Island at 71^{o}N 8^{o}W, ice cover in the Labrador Sea during the 1960s was below normal (Figure 2). In 1971 a reduction in ice in the Odden was accompanied by a procession of positive ice anomalies extending through Denmark Strait, along the Greenland coast, around Cape Farewell and into the Labrador Sea where sea ice increased in 1971 and particularly in 1972 in the region to the south and east of the mean East Greenland SIC. In 1983 and 1984 and again in 1991 and 1993 reductions in SIC to below normal levels in the Odden were mirrored by large increases in SIC in the Labrador Sea, particularly over the deep basin south of 65^{o}N and covering an area of as much as $2x10^{5}$ km^{2} (Figure 1). By 1995 SIC anomalies in the Odden and the Labrador Sea had largely reverted to the levels seen in 1960, with ice largely disappearing from the Odden region.

Thus, as shown by Deser et al. (2002), there were three major episodes of ice expansion in the Labrador Sea (1972-1974, 1983-1984 and 1991-1993) but these appeared to lag Odden ice formation by about 4 years and

were more closely related to declining phases of the Odden ice (Figure 2). The apparent trail of intermittent high ice anomaly through the Denmark Strait and round Cape Farewell particularly in 1971, 1977 and 1983 implies an export of ice and meltwater from the Odden to the Labrador Sea, raising the possibility that SIC increases in the Labrador Sea could be linked to the periodic release of ice and meltwater from the Odden.

North of Denmark Strait the trail of high ice anomaly appears to follow the ice edge (e.g.1977) but further south it clings to the normal route of ice and meltwater close to the coast of East Greenland. Thus, the overall significance of Figure 2 is to demonstrate a transfer of positive ice anomaly (blue) from the Odden region to the Labrador Sea on three occasions between 1970 and 1990 and that south of Denmark Strait, these ice transfers utilize the normal route of ice transport on the East Greenland shelf.

This idea is supported by the results shown in Figure 3a which gives a more quantitative comparison of the amounts of sea ice in the Odden and the Labrador Sea in February between 1960 and 2000. Areas corresponding to these two sites were selected from Figure 1 (boxes) based on the maximum area anomaly of Labrador Sea ice (1983) and of Odden anomaly (1969). February was chosen because this was generally the month giving the highest Odden SIC. Consistent with results shown in Figure 2 there were three major periods of high ice fraction in the Odden region of the GIN, 1967-70, 1977-79 and 1985-89 with a smaller peak in 1997-98 (Figure 3a). The temporal changes in Odden ice are similar to those reported by Rogers and Hung (2008) and Niederdrenk and Mikolajewicz (2016), which showed major peaks in the 1960s, 1977-80, 1985-88 and 1997. The smaller peak in 1997-98 (Figure 3a) may have been different from the three main peaks because according to Wadhams and Comiso (1999), Odden ice in this period contained a large proportion of older ice. After 2005 only small transient peaks were evident (not shown).

Ice fraction in the Labrador Sea was generally low when Odden ice cover was high (e.g. 1999, 1977-1979, 1986, 1990-1991 and 1997-1998) and the three well-defined Labrador Sea peaks (centered on 1972, 1983-1984 and 1993 as described by Deser et al. 2002) were about 4-5 years later than the Odden peaks as confirmed by lag analysis (correlation coefficient is maximum, r= 0.42). These Labrador Sea peaks occurred when the Odden was in a declining phase (1970-74, 1983-85 and 1987-95), consistent with a possible link between Odden meltwater and Labrador Sea SIC. Mysak and Manak (1989) also found a lag of about four years between ice maxima in the Greenland and Labrador Seas.

Figure 2. Anomalies (relative to mean for 1960-2020) of February mean sea ice cover (SIC, HadISSTv2.2) in the GIN and Labrador Seas for selected years between 1960 and 2000. White areas east and west of Greenland indicate where SIC is very high (>0.9) and changes little from year to year. Grey line indicates the ice front (0.2 ice cover fraction). Vertical scale is SIC anomaly calculated relative to the mean values between 1960 and 2020. Pale yellow denotes either land or open sea while the white regions signify no substantial anomaly of normal ice cover or 100% ice cover. Boxes in the 1960 map indicate the two areas chosen for analysis in Figure 3: Labrador Sea 'L' 70°-75°N to 15°W to 5°E and Odden ice feature 'O' 55°-65°N 60°-50°W.The GIN Sea is the area east of Greenland, north of Iceland, west of Norway and south of 80°N (Svalbard) (Figure 1).

Figure 3. The relation of sea ice cover (SIC) and SST anomalies (based on 1960-2020 mean values) in the Odden region and Labrador Sea to land temperature anomalies in East and West Greenland. (a). February SIC (1960-2000) in the Odden region (70°-75°N to 15°W to 5°E) and in the southern Labrador Sea (55°-65°N 60°-50°W) (see boxes in Figure 1.) (b) Temperature anomaly in the Odden and Labrador Sea as in (a). January land temperatures (see Data and Methods and Open Research sections) are shown in (c) at Ilulissac (69°N 51°W) and Qaqortoq (60°N 46°W) in West Greenland and in (d) at Ittoqqortoormiit (70°N 22°W) in E. Greenland and in Svalbard (78°-79°N 14°-18°E); (e) (f) February temperature anomaly time series (CRU TS see Data and Methods) in (e) the Labrador Sea (55°-65°N 60°-50°W)compared with SW Greenland (62°-67°N 50° -45°W)(SW in Figure 1) and (f) E. Greenland (70°-75°N 30°-25°W)(area E in Figure 1) compared with the Odden region (70°-75°N 15W°-5°E). (b-f) are plotted with reversed sign to compare with SIC (a). The positions of Ilulissac (Ilu), Qaqortoq (Q), Svalbard (S) and Ittoqqortoormiit (Itt) are indicated in Figure 1.

Figures 2 and 3a both indicate three major increases in ice in the Labrador Sea (1972, 1983 and 1991,1993) after reductions in ice in the Odden region of the GIN. The rise in these years matches the declines in Odden ice in 1970-72, 1980-81 and 1987-90 respectively with a lag of about 1-3 years and not the 4-5 years between peaks of SIC in the Odden and those in the Labrador Sea. Temperature anomalies in the Labrador Sea (Figure 3b) follow the pattern of Labrador Sea SIC anomalies in (a) (correlation coefficient r = 0.74, 1960-2000),. Correspondence between SIC and SST anomalies is good for the 1960s peak of Odden ice but less so for the subsequent Odden peaks.

The differences in SIC time series between the Odden and the Labrador Sea in Figure 3a are mirrored by differences in land air temperatures on each side of Greenland (Figures 3c,d). The time series for SIC in the Labrador Sea (Figure 3a) resembles those for land temperatures at Ilulissac (69^{o}N 51^{o}W) and Qaqortoq (60^{o}N 46^{o}W) which are very similar (r=0.92, Figure 3c) despite these stations being 1000 km apart on the west coast of Greenland. Likewise, the temperature time series at Ittoqqortoormiit on the east coast (70^{o}N 22^{o}W) and at Svalbard 1500km across the GIN Sea (Figure 3d) look similar (r = 0.71 from 1960-2000) and comparable to the Odden SIC time series in Figure 3a. Three major peaks of Odden SIC (Figure 3a) correlated with three temperature troughs at Ittoqqortoormiit (Figure 3d) (r = 0.52 between 1960 and 2000) and Svalbard (Figure 3d), (r = 0.46). Three peaks of SIC in the Labrador Sea (Figure 3a) correlated with three temperature troughs at Ilulissac (3c) (r = 0.73, 1960-2000) and Qaqortoq (Figure 3c) (r = 0.72, 1960-2000). All these correlation coefficients are comfortably within the 95% confidence level.

Because the high ice anomaly in the Labrador Sea extended to the Greenland coast (Figure 2, 1971-72, 1983-1984 and 1991-1992) we considered the possibility that unusually cold temperatures in Greenland might be key to the formation of the anomalous ice. This idea was tested by comparing HadISST in the freezing area (55^{o}-65^{o}N 60^{o}-50^{o}W) with air temperatures in SW Greenland (CRU TF, Figure 3e). The results showed a convincing correspondence between these two parameters (r=0.61 1960-2000) and this inferred that cold air from SW Greenland was a major determinant of ice formation in the Labrador Sea. Correlation of SW Greenland air temperature with SIC in the Labrador Sea (Figure 3a) was r = 0.64. Similarly, there was a correspondence between HadISST in the Odden region and land air temperature (iCRU4) in East Greenland (Figure 3f) although not so convincing (r=0.4) and similar to the correlation between Odden SIC and East Greenland air temperature (r=0.45).

No marked Labrador Sea peak of sea-ice was observed around 2000 despite the well-defined peak of Odden ice seen in 1997 (Figure 3a) but in this case air temperatures in coastal West Greenland did not attain the extreme cold levels seen during the three main Labrador Sea ice expansions (Figure 3c). It is likely that Labrador Sea ice expansion between 1960 and 2000 required both an input of cold fresh water and ice from the Odden and local extreme low temperatures in the Labrador Sea. Wadhams and Comiso (1999) found that the 1997 Odden ice was seen late in the spring and had a high proportion of thick ice advected from the E. Greenland Current so it was not typical.

2. The relationship between Odden SIC and Arctic sea-level atmospheric pressure (SLP)

As noted in the Introduction, several studies have linked high SLP in the Arctic to increased transport of ice through Fram Strait (Dickson et al. 1985; Mysak and Manak (1989); Köberle and Gerdes 2003; Tsukernik et al. 2010) and increased sea ice in the region of the GIN Sea corresponding to the Odden (Hilmer et al. 1998; Rogers and Hung 2008; Germe et al. 2011). This connection is supported by the observations shown in Figure 4a which confirm that in winter of the years 1960 to 2000 there is a clear correspondence between Odden SIC (at 70^{o}-75^{o}N 20^{o}W-5^{o}E) and Arctic SLP at 85^{o}N 30^{o}W (north of Greenland, Figure 1). Notably there are three major periods of high SLP north of Greenland which can be related to peaks of Odden SIC (maximal in 1968-70, 1976-79 and 1986-89 and similar to those described by Rogers and Hung 2008). In contrast, the Arctic Oscillation Index (AOI) was inversely related to Odden ice and SLP with major troughs aligned with high Odden ice and SLP in 1969, 1977 and 1986. Between 1965 and 1995 correlation between SIC and AOI was r = -0.38 but correlation between SIC and SLP was r = +0.54 (both values >95% confidence) so high SLP north of Greenland is a more useful pointer to Odden ice formation than the AOI.

In December to February of high Odden years (1969, 1978 and 1986) pressure was high over Greenland whereas in low Odden years (1976, 1984 and 1993) low pressure over Iceland and Scandinavia was the predominant feature (Figure 4b). This appears similar to the demonstration by Tsukernik et al. (2010) of a SLP dipole governing the movement of ice through Fram Strait. High SLP over Greenland and low pressure over Scandinavia would channel northerly winds through Fram Strait which are likely to promote sea ice transport out of the Arctic and to cool the GIN Sea and encourage new ice formation there (Hilmer et al. 1998). High pressure over Greenland would channel southerly winds up the Labrador Sea which would inhibit ice formation and contribute to the observed reciprocal temperature regimes between East and West Greenland (Figure 3c,d). It might also favour subsidence of very cold still air from the Greenland ice cap over the coastal waters east of Greenland.

Figure 4. (a) Time series for Odden SIC (HadISST2;70°-75°N to 15°W-5°E), Arctic SLP at 85°N 30°W and Arctic Oscillation Index (AOI) for February of each year between 1960 and 2000. SLP values (ERA5) are presented as hPa and AOI as AOI index/10 to aid comparison with SIC. (b) North polar stereographic latitude-longitude plot of December to February mean SLP between 65°N-85°N and 70°W-20°E in high Odden ice years (1968-69, 1977-78, 1985-86) and low Odden ice years (1975-76,1983-84, 1992-93).

Figure 5. Anomalies (relative to 1960-2020) of HadISST (sea surface temperature) track the transfer of cold water from the GIN Sea along the Greenland coast and into the Labrador Sea in February, June and November of 1969,1982 and 1989. The white regions represent either the landmasses of Greenland, Iceland or Labrador or ice extending away from the coast of these regions.

3. The trajectory of Odden meltwater and its effect on sea-ice formation in the Labrador Sea.

The periods of declining Odden ice involved the release of ice-laden, cold low-salinity water which appeared to be routed through Denmark Strait, along the SE Greenland coast and round Cape Farewell into the Labrador Sea (Figure 2). To follow the fate of cold fresh water released from the declining Odden we used HadISST1 sea surface temperature data (Figure 5). In the February of 1969,1982 and 1989 there was a pronounced negative SST anomaly north of Iceland corresponding to the Odden region. In 1969 this did not extend into the Labrador Sea but it did in 1982 and 1989. By June of each year a trail of cold water followed the coast of East Greenland and into the Labrador Sea. In November of these years there was an intensification of cold water in the Labrador Sea in an area which corresponded to ice formation in the following winter (Figure 2) but extending further south into the SPG region. It may be significant that particularly in 1982 there was a band of anomalously warmer water which followed the East Greenland coast and the ice edge north of 70°N. This warm anomaly was distinct from the trail from the Odden which by the following April extended into the Labrador Sea via a narrow band (about 100 km wide) of cold water extending from the Denmark Strait along the East Greenland shelf break.

There are several estimates of the velocity of the boundary current from Denmark Strait to Cape Farewell and these are all in the region of 0.3-0.5 m/sbut there is little information north of 70°N although the velocity appears to be much slower (Fratantoni 2001, Flatau et al. 2003, Reverdin et al. 2003). Assuming a mean figure of 0.2m/s between the Odden and Cape Farewell (about 2500km), the transit time of temperature/salinity anomalies would be about 4-5 months which is in reasonable agreement with the June to November time scale suggested by Figure 5. Overall, these findings are consistent with the hypothesis that meltwater and ice from the declining Odden were routed through Denmark Strait, along the East Greenland coast and into the Labrador Sea where potentially they could have facilitated ice formation (Close et al. 2018) in the winters of 1970-72, 1983-1984 and 1991-93 (Figures 2,3).

4. Cold fresh water in the southern Labrador Sea predates and postdates ice formation

If cold fresh water from the Odden enters the Labrador Sea and creates conditions which favor ice formation in winter, then there should be evidence of such a water layer which predates ice formation. Thus Deser et al. (2002) showed that a drop in April-July salinity predated ice formation in the Labrador Sea in the following winter. We chose to investigate the area 58°-65°N 60°-52°W (the region of anomalous ice in the

Labrador Sea seen in Figure 2) and compared changes in anomalies of 0-400m salinity (S400) (a) and ocean heat content (OHC400) (b) with sea ice cover (SIC) between 1970 – 1995. This period included all three of the high ice periods in the Labrador Sea, 1971-77, 1983-85 and 1989-94 (Figure 6a,b).

We gave most attention to the period 1982-1985 which included the largest and least complex ice expansion events. There was a small ice peak in the winter of 1982 but much larger peaks in 1983 and 1984 each of which were preceded by a large decrease in salinity anomaly (Figure 6a) in the Labrador Sea which was greatest in August 1982 (vertical dashed line X) and August 1984 (vertical dashed line Y). The 1982 freshening probably represents the increase in fresh water reported by Deser et al. (2002) and most likely corresponds to the initial influx of cold fresh water from the Irminger Sea (Figure 5) representing the start of the GSA. The pronounced **increase** in salinity anomaly between September and November 1982 cannot be connected with ice formation, which did not commence until December, but may have been associated with mixing and southwards dispersal of the original influx of fresh water. Only a small decrease in Labrador Sea salinity was seen in August 1983 and could represent a smaller new fresh water influx from the Irminger Sea or perhaps some meltwater from the 1983 ice.

There was a second large decrease in salinity by August 1984 which was similar in magnitude to the initial changes in 1982 and was most likely to correspond to the meltwater from the ice formed in the winter of 1984 (dashed line Y). Increase of salinity from August to December 1984 is presumed to correspond to movement of this meltwater southwards and out of the Labrador Sea. Thus, it appears that there was an approximately two year period between the initiation of the GSA by influx of Odden meltwater into the Labrador Sea in summer 1982 and the appearance of meltwater from Labrador Sea ice in summer 1984. Dispersal southwards into the SPG would have occurred after that. The pattern of change in OHC anomaly (Figure 6b) resembled that for SST (Figure 6c) and was similar to that of salinity anomaly with the largest troughs corresponding to summer 1982 (influx of cold water from the Irminger Sea) and the fall of 1984 (efflux of cold meltwater from the Labrador Sea). There may have been a small decrease in OHC anomaly in summer 1983 (as for salinity, Figure 6a) but this was subsumed within a higher baseline during 1983.

Interpretation of the changes in salinity and OHC between 1970-80 and 1985-95 was more complicated because of the succession of years with smaller increases in winter ice during these periods and the consequent difficulty in distinguishing between influx of meltwater from East Greenland and meltwater from the Labrador Sea ice. However, it seems clear that there were sharp decreases in salinity anomaly in the summers before and after winter ice formation in 1972-74, 1989-91 and 1992-93 which were analogous to those seen in 1982-84. Comparable changes were also seen in OHC anomaly (Figure 6b). The correlation coefficient for S400 versus OHC400 was 0.66 (>95% confidence) between 1965 and 1995, confirming that these two independent parameters showed quite similar changes over this period as expected if they reflected mass changes involving the movement of tranches of cold fresh water.

Figure 6. The relation between fractional sea-ice cover (SIC) and anomalies of (a) 0-400m salinity (S400) (psu x4), (b) 0-400m ocean heat content (OHC)(GJ/m^2) and (c) ERA5 surface heat flux anomaly (GJ/m^2, positive anomalies downwards) and HadISST SST anomaly (^{o}C) in the Labrador Sea between 58^o-65^{o}N and 60^o-52^{o}W from 1970 to 1995. Anomalies are relative to 1981-2010 mean monthly climatology. Dashed lines X and Y highlight August 1982 and 1984 in (a) to (c).

We considered the possibility that some of the variation in the results for OHC (Figure 6b) was due to changes in surface heat flux anomaly (Figure 6c – downward flux anomalies are positive). There is a weak inverse relationship between SST and downward net heat flux anomalies (r= −0.26) indicating more surface heat loss with anomalous warming and implying that surface heat fluxes anomalies are not driving SST changes (Figure 6c). Instead, it seems likely from the data between 1982 and 1985 that the periods of higher downward heat flux anomaly coincided with the periods of high SIC in winter i.e. high ice cover inhibited loss of ocean heat. In September 1982-1985) when negative anomalies of heat and salt were greatest and there was no sea ice (Figures 6a, b) values for downward heat flux anomalies were very low (in the range ±0.02 GJ/m^2) and trivial compared with the corresponding values for OHC (about 2 GJ/m^2, Figure 6b). As expected, the pattern of changes in OHC (Figure 6b) resembled that of SST (Figure 6c) and it is notable that the mean temperature of the 400m layer indicated by the OHC values (1982-1985, 2 GJ/m^2) in Figure 6b is about -1.2^{o}C (calculated using values for density of sea water of 1027 kg/m^3 and heat capacity of 4003 J/kg/K) which is close to the mean SST values in Figure 6c (1982-1985, -1.4^{o}C). This suggests the mixed layer depth is a substantial fraction of the 400m layer considered at this point and time in the Labrador Sea

and that observed changes in surface heat flux would be even less significant compared with the temperature of a layer of this thickness. From the results shown in Figure 6 we conclude that accumulation of unusually cold, low salinity water in the southern Labrador Sea during the summers of 1971, 1982 and 1989 was likely to have provided the basis for the increases in SIC in the winters of 1972, 1983-84 and 1990 in accordance with the hypothesis of Close et al. (2018). Melting of this ice in each case was associated with a subsequent decrease in salinity and OHC which was of a similar order of magnitude to the initial decrease caused by influx of Odden meltwater.

5. Surface temperature anomalies in the SPG during the 1980s GSA

To further identify the cold fresh water entering the Labrador Sea in June-August 1982 at the start of the GSA (Figure 6), we examined the path of this water around the SPG to enable a comparison with the classic pattern described by Belkin et al. (1998) and Belkin (2004). Because it represented the largest and least complicated GSA event based on SIC fraction and SST anomalies (Figure 3a,b), we restricted our analysis to the freshening and cooling event which began in the fall of 1982 and ended in 1985 (Figure 6). Latitude-longitude plots of changes in salinity and OHC 0-400m were too low resolution (1^o) to pick out a GSA path which had originally been defined by weather stations and moorings at precise locations (Belkin et al.1998).

However, we did obtain useful information using OISST data (Figure 7) which resolves to 0.25^o in latitude and longitude although of course it only gives information about surface temperature conditions. The Great Salinity Anomalies were also Great Temperature Anomalies (Belkin et al. 1998, Belkin 2004) so it is reasonable to examine the use of OISST anomaly data to monitor the progress of the GSA from the Labrador Sea and around the SPG. Also, HadISST data were useful in following the path of meltwater from the Odden (Figure 5) and the HadISST time series (Figure 6c) largely followed that for salinity data in Figure 6a. We divided the data into three phases: Figure 7a which follows the path of cold water derived directly from the influx of Odden meltwater and breaking out into the SPG in the fall of 1982 (the beginning of the GSA) before the major freezing episodes in the Labrador Sea in 1983 and 1984; Figure 7b which covers a period in 1983 when cold water was substantially retained in the Labrador Sea and Figure 7c which follows the outbreak of meltwater derived from the frozen Labrador Sea in late 1984 and represented the end of the GSA.~~.~~

On September 1st 1982 when cold water from East Greenland had reached the southern Labrador Sea (Figure 7a) the SPG was largely occupied by warm anomalies apart from near the Tail of the Grand Banks (TGB). By October 1st there were much increased surface cold anomalies in the Labrador Sea, breaking out into the northern SPG region. This sudden influx of cold water into the SPG is most likely to represent the start of the GSA initiated by entry of Odden meltwater into the Labrador Sea in June-August 1982 (Figure 6). By December, these cold anomalies had spread over the entire SPG and beyond while cold anomalies in the Labrador Sea diminished, consistent with a movement of cold fresh water accumulating in the Labrador Sea and passing into the SPG. By March 1983 warm anomalies had returned to the SPG but cold anomalies remained strong in the southern Labrador Sea, which by then was largely ice-covered (Figure 2). ~~)~~. The warming coincided with anomalously positive heat fluxes into the ocean over much of the North Atlantic region during February 1983 (up to 200 Wm^{-2} around 50^oN, 40^oW) linked to warm, southerly winds to the east of low pressure around 45^oW, 45^oN (not shown). The heat fluxes clearly cannot explain the cold, fresh water accumulating in the Labrador sea where instead the sea-ice cover reduced heat flux loss to the atmosphere. We conclude that although some of the fresh cold water of the 1982 GSA remained in the Labrador Sea where it froze in the 1982-83 winter, a large amount overflowed into the SPG in the fall of 1982. The dramatic changes in OHC400 and S400 in the Labrador Sea seen in summer 1982 (Figure 6a,b) can then be seen to reflect the transit of a layer of cold water into the Labrador Sea which then broke out into the SPG in the fall.

For more than a year between March 1983 and September 1984 cold anomalies (including the residue of the 1983 cold, fresh water influx and 1984 winter ice) remained in the Labrador Sea and mostly warm anomalies occupied the SPG (Figure7b). There was an exception to this regime in October 1983 when cold anomalies moved southwards, perhaps corresponding to the minor trough of salinity in September-October 1983 (Figure 6a). This accumulation of cold fresh meltwater in the Labrador Sea is registered as the second trough of OHC400 and S400 anomaly in September 1984 (Figure 6a,b).

In October 1984 there were profound changes in the distribution of cold surface water with an apparent flood of cold anomalies out of the Labrador Sea (Figure 7c). This cold breakout accounts for the steep decrease in salinity and OHC anomalies in the Labrador Sea after September 1984 (Figure 6a,b). By December 1st 1984 (Figure 7c), cold anomalies were most predominant in the SPG and were distributed in the Labrador Sea (1) Labrador Current (2), near the TGB (3) east of Flemish Cap (4), around Northwest Corner (5) and towards the CGFZ (6) (see Figure 1). In the following months up to February 1st 1985 the cold anomalies in the SPG faded (apart from along the line of the Labrador Current) and warm anomalies returned to the East Greenland coastal region. This represented the end of the 1980s GSA in the SPG and fits the conclusion of Belkin (2004) that the GSA was prominent in the SPG between 1982 (October, Figure 7a) and the beginning of 1985 (Figure 7c).

These results are consistent with an influx of cold water into the Labrador Sea from East Greenland in the latter part of 1982 (some of which circulated around the SPG, Figure 7a), the freezing of this water layer in the winters of 1983 and 1984, the eventual outbreak of the cold meltwater into the SPG in the fall of 1984 and its subsequent dispersal in early 1985.

We wondered if surface heat flux anomalies might be responsible for some of the changes in OISST anomalies shown in Figure 7. Two different situations were considered: (1) August of 1982 and 1984, before the breakout of cold water from the Labrador Sea into the SPG in those years and (2) September 1982 and October 1984 during the breakouts. At these times of the year there was no sea-ice to complicate the interpretation. As in Figure 6c, in August of both years there were low and variable surface heat flux anomalies (defined as positive downward) associated with the colder waters in the Labrador Sea. In contrast, in September of 1982 and October of 1984 when breakout of cold SST anomalies into the SPG had occurred (Figure 7a,c), large negative downward (i.e. upward) heat flux anomalies appeared in the SPG. There was a difference between the wind patterns in August and October as judged from the SLP isobars: in August the mean wind fields were westerly and light whereas in September/October they became north-westerly and stronger so these winds could have been responsible for transfer of heat to the atmosphere even from anomalously cold water surfaces. Such winds would also have the mechanical effect of facilitating the transfer of cold meltwater from the Labrador Sea into the SPG. The accompanying strong easterly winds south of Greenland may also have assisted the movement of water from the Greenland shelf into the Labrador Sea.

The magnitude of the upward surface heat flux anomaly in the western SPG region (40-50^{o}W, 50-60^{o}N) was 43 Wm^{-2} in September 1982 and only 23 Wm^{-2} in October 1984 (when heat loss was stronger in the NAC region to the south east) and with both months influenced by cold, northwesterly airflow as implied by the surface pressure patterns. An anomaly of 40 Wm^{-2} is equivalent to about 0.1 GJ/m^2 integrated over a month, greater than the variations seen in the Labrador Sea (Figure 6c) and more than an order of magnitude less than the OHC change seen in Figure 6b (about -2.5 GJ/m^2). This heat loss can be assumed to cool the upper mixed layer ocean which in this region ranges from 15-58 m (5th – 95th percentile range) in September and 22-88 m in October based on the Johnson & Lyman (2022) climatology, consistent with previous estimates (de Boyer Montégut et al. 2004). It is reasonable to expect a deeper mixed layer during the windy, more turbulent conditions of September 1982 and October 1984. Assuming a mixed layer depth of 50 m, density of sea water of 1027 kg/m^3 and heat capacity of 4003 J/kg/^{o}K, a 0.1 GJ of anomalous heat loss would translate to a slab ocean cooling of less than 0.5^{o}C, much smaller than the observed changes in SST. Therefore, we conclude that although not negligible, the surface fluxes can only explain a small fraction of the SST changes during September-October 1982 and 1984.

Figure 7. The distribution of cold surface water between the Labrador Sea and the SPG on the first day of selected months during the 1982-85 GSA. Latitude plots of OISST anomaly (1981-2010 baseline) followed the distribution of cold surface water between the Labrador Sea (a) in the initial period after the start of the GSA in the fall of 1982 (b) during 1983-1984 and (c) at the end of the GSA in the fall of 1984 and winter of 1984-1985. In (d) are shown the surface net downward heat flux anomalies and SLP (ERA5) for August in 1982 and 1984 (before cold water breakout from the Labrador Sea) and September for 1982 and October 1984 (during cold water breakout). Stations on the SPG are numbered 1-6 in November 1984 and correspond respectively to the Labrador Sea (1), Labrador Current (2), TGB (3), east of Flemish Cap (4), Northwest Corner (5) and the CGFZ (6) according to the schemes of Belkin (2004) and Rossby (1996) as outlined in Figure 1.

Discussion

1. The significance and origin of the Odden ice feature

This work builds on previous evidence that the three Great Salinity Anomaly GSA events which sent anomalous tranches of cold fresh water into the Labrador Sea and around the SPG in the last decades of the 20th century arose originally from increases in ice transport out of the Arctic Sea through Fram Strait (Dickson et al. 1988; Aagaard and Carmack 1989; Hilmer et al. 1998; Häkkinen 1993; Belkin et al. 1998; Schmidt and Send, 2007; Tsukernik et al. 2010). We propose that an important intermediate stage in this process was the formation of the Odden ice feature in the deep basin of the GIN Sea in certain years and that three periods of dissolution of the Odden ice led to three episodes of ice expansion and dissolution in the Labrador Sea and to the three major GSAs. Odden ice provided a subsidiary reservoir of cold fresh water which was secondary to Arctic ice, established a different temperature regime between Eastern and Western Greenland (Figure 3) and eventually reached the SPG as the three GSAs (Figure 7).

Expansion of the Odden could have been initiated by an increase in export of older ice through Fram Strait (Hilmer et al. 1998; Schmith and Hansen 2003; Smedsrud et al. 2017; Wadhams and Comiso 1999; Tsukernik et al. 2010). The time series for ice export through Fram Strait reported by Smedsrud et al. (2017), particularly for March to August, appears to approximate the time series of Odden ice cover between 1960 and 2000 (Figure 2a). However, it was discovered by Wadhams and Comiso (1999) that Odden ice was distinctly different in character from advected ice originating in the Arctic (see Introduction); not only was Odden ice produced in situ thermodynamically but it was labile and could undergo repeated cycles of freezing and thawing (Shuchman et al. 1998).

Observations presented here (Figure 4) strongly associate the creation of the Odden with unusually high SLP to the north of Greenland, consistent with the predictions of the ocean-ice model of Hilmer et al. (1998) that this area of high SLP promoted wind-driven transport of ice out of the Arctic, through Fram Strait (and into the GIN Sea where it formed thick ice in the Odden region. However, strong winds from the Arctic are also likely to increase SIC thermodynamically through anomalous heat loss via turbulent fluxes quite apart from advective ice transport from the Arctic. It may also be necessary to take into account a possible link between high SLP north of Greenland and increases in Arctic ice volume which could have predated enhanced transport of ice through Fram Strait (Köberle and Gerdes 2003, Schweiger et al. 2019).

Odden ice expansion was associated with unusually low temperatures in East Greenland which has a very different temperature regime from West Greenland (Figure 3). Thus, even without taking account of the effect of Arctic winds through Fram Strait, cold air from Greenland also may have an influence on ice formation in the Odden as originally suggested by Shuchman et al. (1998). Increased exit of thick Arctic ice through Fram Strait is likely to expand the East Greenland shelf sea-ice, extending the reach of cold air descending from the Greenland icecap to the GIN Sea.

2. The connection between the Odden ice and the Labrador Sea ice

There was a large initial accumulation of Odden ice in the decade up to 1969 and although there were subsequent increases in SIC around 1977 and 1987, these were on a smaller scale than the original 1960's ice expansion (Figures 2, 3a). In contrast, there is no evidence for substantial interannual changes in the amount of seasonal sea ice on the East Greenland shelf where Comiso et al. (2001) found fairly constant maximum values around 500,000 km^2 between 1978 and 1998. Each of the three main Odden expansions led to Labrador Sea ice expansions about 4-5y later (Figure 3a) but more likely it was transport of ice and fresh water from the decaying Odden to the Labrador Sea after 1969, 1979 and 1986 which promoted enhanced ice cover in the Labrador Sea in 1972-4, 1984-85 and in the early 1990s. This picture accords with the evidence of Close et al. (2018) that pulses of fresh water from the Irminger Sea enhanced ice formation in the Labrador Sea (see Introduction) except that we conclude that the primary source of the cold fresh water was melting of the Odden ice in summer.

Although we provide good evidence here that the melting Odden provides cold water and ice to the Labrador Sea which facilitate ice expansion in the 1970s,1980s and 1990s (Figure 2), it has not been clear to what extent freezing depends on unusually low temperatures in the Labrador Sea. Despite the paucity of air temperature data for central Greenland the limited evidence suggests that there is a clear connection between

unusually low air temperatures in SW Greenland and unusually low SST in the Labrador Sea which would certainly increase ice formation. Although it has been mooted in the past that cold air from Labrador or Baffin Land might freeze the southern Labrador Sea, there is a clear relationship between ice expansion and extreme Greenland air temperatures (Figure 3e). Thus, we suggest that cold fresh water from the Odden and cold air from SW Greenland both contribute to periods of increased SIC in the Labrador Sea.

3. The connection between the Odden and the GSAs

Although it was initially proposed that the GSAs originated in Arctic ice exported through Fram Strait and transmitted down the eastern coast of Greenland, around Cape Farewell and into the Labrador Sea (Introduction), our findings make it more likely that the intermediate origin of the GSAs was the Odden ice which represents a more transient and labile reservoir of fresh water than ice transported through Fram Strait into the East Greenland Current. Crucially, three dissolutions of Odden ice preceded three major freezing events in the southern Labrador Sea (Figure 1, 2a) and the three GSAs in the 1970s, 1980s and 90s (Belkin et al. 1998).

Figures 2,5 and 6 strongly suggest that in the years prior to ice expansion in the Labrador Sea, cold surface water and ice originating in the Odden region passed through the Denmark Strait, along the East Greenland coast and into the Labrador Sea where it formed a pool of cold fresh surface water in the spring/summer seasons which would have conditioned the southern Labrador Sea for enhanced ice formation in the following winter (Close et al. 2018). The maximum area of the Odden after 1979 was about $3x10^5$ km^2 according to Shuchman et al. (1998) and Comiso et al (2001). For 1969 we estimate an area of about $4x10^5$ km^2 from Figure 1 and assuming an average ice thickness of 1m (Selyuzhenok et al. 2020) this would be equivalent to about 400 km^3 of fresh water (not accounting for the lower density of ice). Wadhams et al. (1996) found substantially lower thicknesses (< 0.3m) but their samples were taken in April at the end of the freezing period in a year (1993) when ice cover in the Odden was in a declining phase (Figure 3). The ocean-ice model of Hilmer et al. (1998) predicts thicknesses of Odden ice approaching 4 m and our calculation of fresh water released from the Odden does not take into account the probability of several cycles of freezing and thawing of the Odden over a single year, which would contribute additional fresh water (if the brine sinks after freezing) nor the observation that the GSAs were spread over more than one year (Dixon et al.1988). Indeed, Shuchman et al. (1998) found that the amount of annual ice generated in the Odden was 2-3 times the maximum area covered, giving a value of 800-1200 km^3 of fresh water which could potentially be released from the Odden in a single year. This estimate agrees well with the value of 1000 km^3 per year calculated by Belkin et al. (1998) based on an approximation by Dickson et al. (1988) for the salt deficit of the 1971-72 GSA. A similar figure was calculated by Curry and Mauritzen (2005) for the extra fresh water added to the North Atlantic for the first GSA in the early 1970s. These values are considerably larger than the normal 620 km^3 appearing in the West Greenland Current between June and August in 1996-2001, after the GSA period (Schmidt and Send 2007). We note that recent estimates of total fresh water equivalent exported through Fram Strait per annum in 1993-2008 were about 2400 km^3 of ice or about 2200 km^3 of water (Spreen et al. 2020; Karpouzoglou et al. 2022) so the GSAs in the last century may represent up to 45% of normal annual Fram Strait export.

If the start of the GSA is defined by the first appearance of cold water in the SPG, then the end of the GSA is marked by the final disappearance of this water from the SPG when there was no longer a reservoir of ice and cold water in the Labrador Sea or the Odden which was available to replenish the SPG. This is clarified for the 1980s GSA from data comparing the distribution of salinity and temperature anomalies around the SPG between 1982 and 1985 (Figures 6,7) which shows that cold fresh water entered the Labrador Sea in summer 1982, **before** the major periods of ice formation in the winters of 1983 and 1984. Some of this cold water distributed around the SPG in the fall of 1982 (Figure 7a) but a large portion was retained in the Labrador Sea where it facilitated ice formation in the winters of 1983 and 1984. Eventually the end of the GSA was reached after February 1985 when cold water finally left the Labrador Sea and gradually disappeared from the SPG (Figure 7c). Thus, the propagation of the 1980s GSA appears to correspond to an influx of Odden meltwater into the Labrador Sea in 1982 followed by two years (1983, 1984) of ice formation, after which the ice melted and the cold fresh anomaly moved southwards out of the Labrador Sea, around the SPG and was then either recycled or dissipated elsewhere at the end of 1985.

We conclude that the 1980s GSA corresponds to entry of Odden meltwater into the Labrador Sea and its redistribution around the SPG because (a) the quantity of notional fresh water potentially released from the

Odden is about 1000-1200 km^3 per year (Schuchman et al. 1998) and is similar to previous estimations of fresh water added by the GSA (Belkin et al. 1998) (b) the timings of beginning (1982) and end (1985) of the 1980s GSA (Belkin, 2004) correspond to the entry into and exit from the Labrador Sea of large quantities of cold fresh water (Figure 6) and (c) the distribution of the cold fresh water around the SPG is consistent with previous determinations of the path of the GSA and follows established currents including the West Greenland, Labrador and North Atlantic Currents. Although the data is more difficult to analyse for 1972 and 1989-90, there are significant similarities between these events and those of the 1980s to infer that they share a common mechanism which links Odden meltwater to the GSAs and the episodes of freezing in the Labrador Sea.

Our findings may also be relevant to the timing of the shutdown of deep convection in the Labrador Sea which occurred around 1970-71 at weather station Bravo (56.5°N 51°W) (Lazier 1980). Gelderloos et al. (2012) attributed this shutdown to increased ocean stratification caused by an influx of cold fresh water from the Arctic through Baffin Bay but the findings presented here make it more likely to derive from the Odden after its dissolution starting in 1969 (Figures 2a, 4a). Bravo is in that region of the Labrador Sea where deep convection is known to occur and also where low-salinity water derived from the Odden might be expected to cause stratification in the early 1970s, 1980s and 1990s leading to enhanced freezing in the Labrador Sea in 1972, 1983-84 and 1990-93 (Figure 5). It is apparent from the work of Yashayaev and Loder (2016) that deep convection along the AR7W line centred on 57°N 52°W was inhibited not only in 1969-72 but also in 1983-85 when unusually low density water formed a cap on the surface layer. However, this appeared not to be true in the 1990s when protracted deep convection took place even throughout the major icing event in 1991-1994. Schmidt and Send (2007) showed that the depth of winter convection in the central Labrador Sea is strongly influenced by the prevailing stratification in late summer and that the source of cold surface water could be traced to East Greenland. The Odden ice may thus not only have influenced deep convection in the Nordbukta (Visbeck et al. 1995; Selyuzhenok et al. 2020) but also in the Labrador Sea as Odden meltwater reached the W. Greenland Current and initiated the GSA and freezing events in the Labrador Sea.

It remains unclear why the Odden appeared during three periods at the end of the 20th century but has been largely absent in the 21st century, with the consequent absence of GSAs or major increases in Labrador Sea ice. Certainly, there was a sudden jump of about 1°C in North Atlantic and Labrador Sea SST around 1995-2000 (Robson et al. 2016) which would have reduced the likelihood of ice formation in the Odden and the Labrador Sea, so it is possible these freezing events will not occur again as the Earth continues to warm.

Conclusion

We provide evidence for a new way of explaining not only the three periods of extensive ice coverage in the Labrador Sea basin in the last decades of the 20th century, but also the three Great Salinity Anomalies (GSAs) observed over the same period. Both these phenomena are consequences of three prior expansions and dissolutions of the Odden ice in the Greenland-Iceland-Norway Sea which led to influxes of summer meltwater into the Labrador Sea where the cold fresh water in conjunction with unusually low air temperatures in Greenland is likely to have facilitated freezing in the following winters. Some of this summer Odden meltwater overflowed into the subpolar gyre where it marked the beginning of the GSA. Subsequent melting of the Labrador Sea ice caused each of three major influxes of cold fresh water into the subpolar gyre which eventually dissipated to mark the end of each GSA. Formation of Odden ice and subsequently of anomalous Labrador Sea ice therefore created subsidiary reservoirs of cold fresh water which reached the Atlantic on a different time scale to the regular direct contribution from Arctic ice.

A wider perspective allows us to trace back the origin of the GSAs to three major peaks of sea ice in the Labrador Sea in 1972, 1983-84 and 1991-93, then to three main Odden ice peaks in 1968-69, 1977-79 and 1986-9, then to three episodes of high SLP in Greenland which introduced strong cold northerly winds driving each of three periods of increased transport of ice from the Arctic through Fram Strait in 1967-68, 1979-80 and 1989 and which appear to have been preceded by three major expansions of Arctic ice volume in 1966, 1980 and 1988. Although the ultimate origin of the GSAs therefore may be traced back to increases in Arctic ice volume about 4-6 years earlier it is possible that these ice volume increases are in turn dependent on atmospheric factors associated with high SLP north of Greenland. These results contribute to our understanding of the links between ocean circulation and ice formation/melt in the North Atlantic, a key component of the climate system.

Acknowledgement Richard Allan received support from the Research Councils UK (RCUK) National Centre for Earth Observation (NE/RO16518/1).

Open research

Sea surface temperature (SST) and sea ice cover (SIC) data were obtained respectively from https://www.metoffice.gov.uk/hadobs/hadisst/ and (https://www.metoffice.gov.uk/hadobs/hadisst2/)

OISST (Optimum Interpolation Sea Surface Temperature) V2 data from the Advanced Very High Resolution Radiometer (AVHRR) infrared satellite were obtained from https://www.psl.noaa.gov/data/gridded/data.noaa.oisst.v2.highres.html . .

Data regarding air temperatures in Greenland coastal sites were obtained from Cappelen, J. (ed.) (2020): Greenland - DMI Historical Climate Data Collection 1784-2019. DMI Report 20-04. Copenhagen. Data for air temperatures in Svalbard were accessed from https://data.giss.nasa.gov/gistemp/. .

Air temperature data CRU TS v4.04 for areas of SW and E. Greenland were obtained from NCAS-Climate, Climatic Research Unit, School of Environmental Sciences, University of East Anglia, Norwich NR4 7TJ (https://crudata.uea.ac.uk/cru/data/hrg/cru_ts_4.07/) as described by Harris et al. (2020).

Data for EN4.2.2 salinity from 0-400m depth (S400) and ocean heat content from 0-400m (OHC400) were obtained from https://www.metoffice.gov.uk/hadobs/en4/ and license for their use are available from http://www.nationalarchives.gov.uk/doc/non-commercial-government-licence/version/2/

Sea level pressure (SLP) data and surface heat fluxes were obtained from https://cds.climate.copernicus.eu/

Arctic Oscillation Index (AOI) data were obtained from https://www.cpc.ncep.noaa.gov/products/precip/CWlink/daily_ao_index/ao.shtml

Initial investigation of dataset listed above were achieved using Climate Explorer (https://climexp.knmi.nl) which is part of the WMO Regional Climate Centre at KNMI (Koninklijk Nederlands Meteorologisch Instituut).

References

Aagaard, K. & Carmack, E. (1989). The role of sea ice and other fresh water in the Arctic circulation. J. Geophys. Res. 94. 14,485-14,498, doi:10.1029/JC094iC10p14485.

Belkin, I. M., Levitus, S., Antanov, J. and Malmberg, S-A. (1998)."Great Salinity Anomalies" in the North Atlantic. Prog. Oceanog. 41 (1): 1–68, doi:10.1016/S0079-6611(98)00015-9.

Belkin, I. M. (2004). Propagation of the "Great Salinity Anomaly" of the 1990s around the northern North Atlantic. Geophys. Res. Letters. 31 (8), doi:10.1029/2003GL019334.

Bower, A.S. and von Appen, W.-J. (2008) Interannual variability in the pathways of the North Atlantic Current over the Mid-Atlantic Ridge and the impact of topography. J. Phys. Oceanog. 38, 104-120, doi:10.1175/2007JPO3686.1.

Bourke, R. H., Paquette, R. G., and Blythe, R. F. (1992), The Jan Mayen Current of the Greenland Sea, J. Geophys. Res., 97(C5), 7241– 7250, doi:10.1029/92JC00150.

Cappelen, J. (ed.) (2020): Greenland - DMI Historical Climate Data Collection 1784-2019. DMI

Report 20-04. Copenhagen.

Close, S., Herbaut, C., Houssais, M.-N. and Blaizot, A.-C. (2018) Mechanisms of interannual to decadal-scale winter Labrador Sea ice variability. Climate Dynamics, 51 (7–8), 2485-2508, doi:10.1007/s00382-017-4024-z.

Comiso, J. C., Wadhams, P., Pedersen, L. T., and Gersten, R. A. (2001), Seasonal and interannual variability of the Odden ice tongue and a study of environmental effects, J. Geophys. Res., 106(C5), 9093– 9116, doi:10.1029/2000JC000204.

Curry, R. & Mauritzen, C. (2005). Dilution of the northern North Atlantic Ocean in recent decades. Science (New York, N.Y.). 308. 1772-4, doi: 10.1126/science.1109477.

de Boyer Montégut, C., G. Madec, A. S. Fischer, A. Lazar, and D. Iudicone (2004), Mixed layer depth over the global ocean: An examination of profile data and a profile-based climatology, J. Geophys. Res., 109, C12003, doi:10.1029/2004JC002378.

Deser, C., Holland, M., Reverdin, G., and Timlin, M. (2002) Decadal variations in Labrador Sea ice cover and North Atlantic sea surface temperatures, J. Geophys. Res., 107(C5), doi:10.1029/2000JC000683.

Dickson, R. R., Meincke, J., Malmberg, S.- A. and Lee, A.J. (1988). The “great salinity anomaly” in the Northern North Atlantic 1968–1982, Prog. in Oceanog., 20,103-15, doi.org/10.1016/0079-6611(88)90049-3.

Flatau, M. K, Talley, L. and Niiler P.P. (2003) The North Atlantic Oscillation, Surface Current Velocities, and SST Changes in the Subpolar North Atlantic. J. Clim. 16(14):2355-2369, doi:10.1175/2787.1.

Florindo-López, C., Bacon, S., Aksenov, y., Chafik, L., Colbourne, E. and Holliday, N.P. (2020) Arctic Ocean and Hudson Bay Freshwater Exports: New Estimates from Seven Decades of Hydrographic Surveys on the Labrador Shelf. J. Clim. 33 (20) 8849–8868, doi.org/10.1175/JCLI-D-19-0083.1.

Fratantoni, D. M. (2001), North Atlantic surface circulation during the 1990's observed with satellite-tracked drifters, J. Geophys. Res., 106(C10), 22067–22093, doi:10.1029/2000JC000730.

Fratantoni, P.S. and McCartney, M.S. (2009) Freshwater export from the Labrador Current to the North Atlantic Current at the Tail of the Grand Banks of Newfoundland. Deep-Sea Research I 57(2) 258-283, doi:10.1016/j.dsr.2009.11.006.

Gelderloos, R., Straneo, F. and Caroline A. Katsman, C.A. (2012) Mechanisms behind the temporary shutdown of deep convection in the Labrador Sea: Lessons from the Great Salinity Anomaly Years 1968–71 J. Climate 25,6743-6755, doi.org/10.1175/JCLI-D-11-00549.1.

Germe, A., Houssais, M.-N., Herbaut, C., and Cassou, C. (2011), Greenland Sea sea ice variability over 1979–2007 and its link to the surface atmosphere, J. Geophys. Res., 116, C10034, doi:10.1029/2011JC006960.

Good, S. A., M. J. Martin and N. A. Rayner, 2013. EN4: quality-controlled ocean temperature and salinity profiles and monthly objective analyses with uncertainty estimates, J. Geophys.Res.: Oceans, 6704 -6716, doi:10.1002/2013JC009067

Haak, H., J. Jungclaus, U. Mikolajewicz, and M. Latif (2003), Formation and propagation of great salinity anomalies, Geophys. Res. Lett., 30, 1473, doi:10.1029/2003GL017065, 9.

Häkkinen, S. (1993), An Arctic source for the great salinity anomaly: A simulation of the Arctic ice-ocean system for 1955–1975, J. Geophys. Res., 98(C9), 16397– 16410, doi:10.1029/93JC01504.

Harris, I., Osborn, T.J., Jones, P. et al. (2020) Version 4 of the CRU TS monthly high-resolution gridded multivariate climate dataset. Sci Data 7, 109, doi.org/10.1038/s41597-020-0453-3.

Hersbach H, Bell B, Berrisford P, et al. (2020) The ERA5 global reanalysis. *Q J R Meteorol Soc*. 146: 1999–2049, doi.org/10.1002/qj.3803.

Hilmer, M, Harder, M and Lemke, P. (1998) Sea ice transport: A highly variable link between Arctic and North Atlantic, Geophys. Res. Lett. 25, 3359-3362, doi.org/10.1029/98GL52360.

Huang, B., C. Liu, V. Banzon, E. Freeman, G. Graham, B. Hankins, T. Smith, and H.-M. Zhang, 2021: Improvements of the Daily Optimum Interpolation Sea Surface Temperature (DOISST) Version 2.1. J. Climate, 34, 2923-2939, doi ; 10.1175/JCLI-D-20-0166.1 (V2.1).

Johnson, G. C., & Lyman, J. M. (2022). GOSML: A global ocean surface mixed layer statistical monthly climatology: Means, percentiles, skewness, and kurtosis. J. Geophys. Res: Oceans, 127, e2021JC018219. doi.org/10.1029/2021JC018219.

Karpouzoglou, T., de Steur, L., Smedsrud, L. H., & Sumata, H. (2022). Observed changes in the Arctic freshwater outflow in Fram Strait. Journal of Geophysical Research: Oceans, 127, doi.org/10.1029/2021JC018122.

Köberle, C. and Gerdes, R. (2003) Mechanisms Determining the Variability of Arctic Sea Ice Conditions and Export, J. Clim. 16,2843–2858, doi.org/10.1175/1520-0442(2003)016<2843:MDTVOA>2.0.CO;2

Lazier, J. R. N. (1980) Oceanographic conditions at Ocean Weather Ship Bravo, 1964–1974, Atmosphere-Ocean, 18:3, 227-238, doi: 10.1080/07055900.1980.9649089.

Lenssen, N., G. Schmidt, J. Hansen, M. Menne, A. Persin, R. Ruedy, and D. Zyss, 2019: Improvements in the GISTEMP uncertainty model. J. Geophys. Res. Atmos., 124, no. 12, 6307-6326, doi:10.1029/2018JD029522.

Mysak, L.A. and Manak, D.K. (1989) Arctic Sea-Ice extent and anomalies, 1953–1984, Atmosphere-Ocean, 27:2, 376-405, doi: 10.1080/07055900.1989.9649342, doi.org/10.1080/07055900.1989.9649342.

Niederdrenk, A. L. and Mikolajewicz, U. (2016): Variability of winter sea ice in Greenland-Iceland-Norwegian Sea in a regionally coupled climate model, Polarforschung, 85 (2), 81-84, doi: 10.2312/polfor.2016.003.

Overland, J. E., and Wang, M. (2005), The Arctic climate paradox: The recent decrease of the Arctic Oscillation, Geophys. Res. Lett., 32, L06701, doi:10.1029/2004GL021752.

Rayner, N. A.; Parker, D. E.; Horton, E. B.; Folland, C. K.; Alexander, L. V.; Rowell, D. P.; Kent, E. C.; Kaplan, A. (2003) Global analyses of sea surface temperature, sea ice, and night marine air temperature since the late nineteenth century J. Geophys. Res. 108 D14, 4407, doi: 10.1029/2002JD002670.

Reverdin, G., Niiler, P. P., and Valdimarsson, H. (2003) North Atlantic Ocean surface currents, J. Geophys. Res., 108(C1), 3002, doi:10.1029/2001JC001020.

Robson, J., Ortega, P. & Sutton, R. (2016) A reversal of climatic trends in the North Atlantic since 2005. Nature Geosci. 9, 513–517, doi.org/10.1038/ngeo2727.

Rogers, J. C. and Hung, M.-P. (2008), The Odden ice feature of the Greenland Sea and its association with atmospheric pressure, wind, and surface flux variability from reanalyses, Geophys. Res. Lett., 35, L08504, doi:10.1029/2007GL032938.

Rossby, T. (1996), The North Atlantic Current and surrounding waters: At the crossroads, Rev. Geophys., 34(4), 463– 481, doi:10.1029/96RG02214.

Schmidt, S. & Send, U. (2007). Origin and Composition of Seasonal Labrador Sea Freshwater. J. Phys. Oceanogr. 37, 1445-1454, doi: 10.1175/JPO3065.1.

Schmith, T., & Hansen, C. (2003). Fram Strait ice export during the nineteenth and twentieth centuries reconstructed from a multiyear sea ice index from southwestern Greenland. J. Climate, 16(16), 2782–2791, doi.org/10.1175/1520-0442(2003)016<2782:FSIEDT>2.0.CO;2

Schweiger, A. J., K. R. Wood, and J. Zhang, 2019: Arctic Sea Ice Volume Variability over 1901–2010: A Model-Based Reconstruction. J. Climate, **32**, 4731–4752, doi.org/10.1175/JCLI-D-19-0008.1.

Selyuzhenok, V., Bashmachnikov, I., Ricker, R, Vesman, A. and Bobylev, L. (2020). Sea ice volume variability and water temperature in the Greenland Sea. Cryosphere. 14. 477-495, doi:10.5194/tc-14-477-2020.

Shuchman, R.A., Josberger, E.G., Russel, C.A., Fischer, K.W., Johannessen, O.M., Johannessen, J. and Gloersen, P. (1998) Greenland Sea Odden sea ice feature: Intra-annual and interannual variability: J. Geophys. Res. (Oceans), 103, 12,709-12,724, doi: 10.1029/98JC00375.

Smedsrud, L.H., Halvorsen, M.H. Stroeve, J.C., Zhang, R. and Kloster, K. (2017) Fram Strait sea ice export variability and September Arctic sea-ice extent over the last 80 years The Cryosphere, 11, 65–79, 2017, doi.org/10.5194/tc-11-65-2017.

Spreen, G., de Steur, L., Divine, D., Gerland, S., Hansen, E., & Kwok, R. (2020). Arctic sea ice volume export through Fram Strait from 1992 to 2014. J. Geophys. Res. (Oceans), 125, e2019JC016039, doi.org/10.1029/2019JC016039

Stendardo, I., Rhein, M., & Steinfeldt, R. (2020). The North Atlantic Current and its volume and freshwater transports in the subpolar North Atlantic, time period 1993–2016. J. Geophys. Res. Oceans, 125, e2020JC016065, doi.org/10.1029/2020JC016065.

Titchner, H. A., and Rayner, N. A. (2014), The Met Office Hadley Centre sea ice and sea surface temperature data set, version 2: 1. Sea ice concentrations, J. Geophys. Res. Atmos., 119, 2864–2889, doi:10.1002/2013JD020316.

Tsukernik, M., Deser, C., Alexander, M. and Tomas, R. (2010). Atmospheric forcing of Fram Strait sea ice export: a closer look. Clim Dyn **35**, 1349–1360, doi.org/10.1007/s00382-009-0647-z.

Visbeck, M., Fischer, J. and Schott, F. (1995) Preconditioning the Greenland Sea for deep convection: Ice formation and ice drift J.Geophys.Res., 100, 18,489 -18,502. doi:10.1029/95JC01611.

Wadhams, P. and Comiso, J. C. (1999) Two modes of appearance of the Odden Ice Tongue in the Greenland Sea. Geophysical Research Letters, 26 (16). 2497-2500, doi:10.1029/1999gl900502

Wadhams, P. and Wilkinson, J.P. (1999) The physical properties of sea ice in the Odden ice tongue, Deep Sea Res. Part II: Topical Studies in Oceanography.46, 1275-1300, doi.org/10.1016/S0967-0645(99)00023-5.

Yashayaev, I., and Loder, J. W. (2016), Recurrent replenishment of Labrador Sea Water and associated decadal-scale variability, J. Geophys. Res. Oceans, 121, 8095– 8114, doi:10.1002/2016JC012046.

Figure 1.

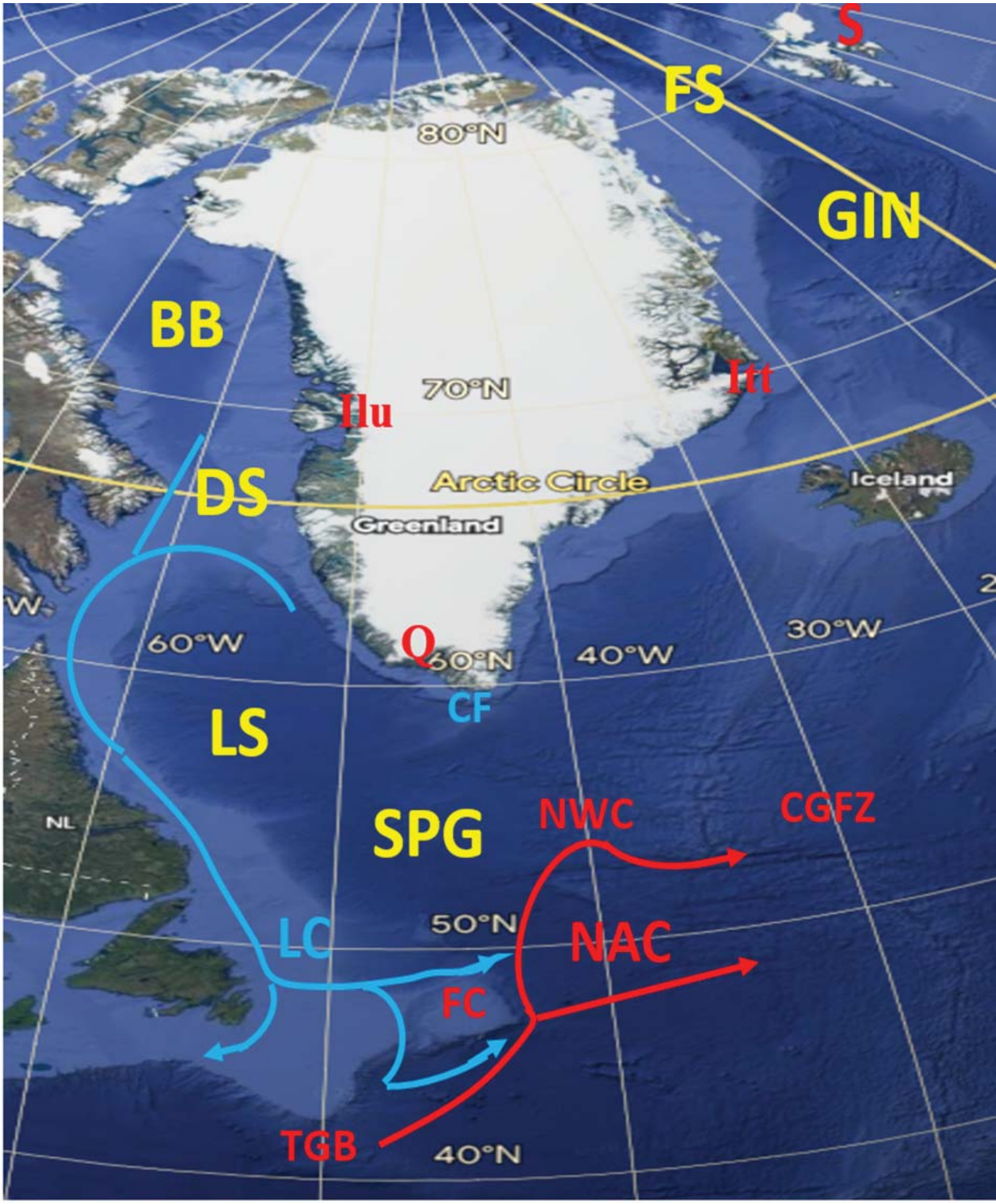
S
FS
80°N
GIN
BB
Itt
70°N
Ilu
DS
Arctic Circle
Iceland
Greenland
W
60°W
Q
60°N
40°W
30°W
CF
LS
NL
SPG
NWC
CGFZ
50°N
LC
NAC
FC
TGB
40°N

Figure 2.

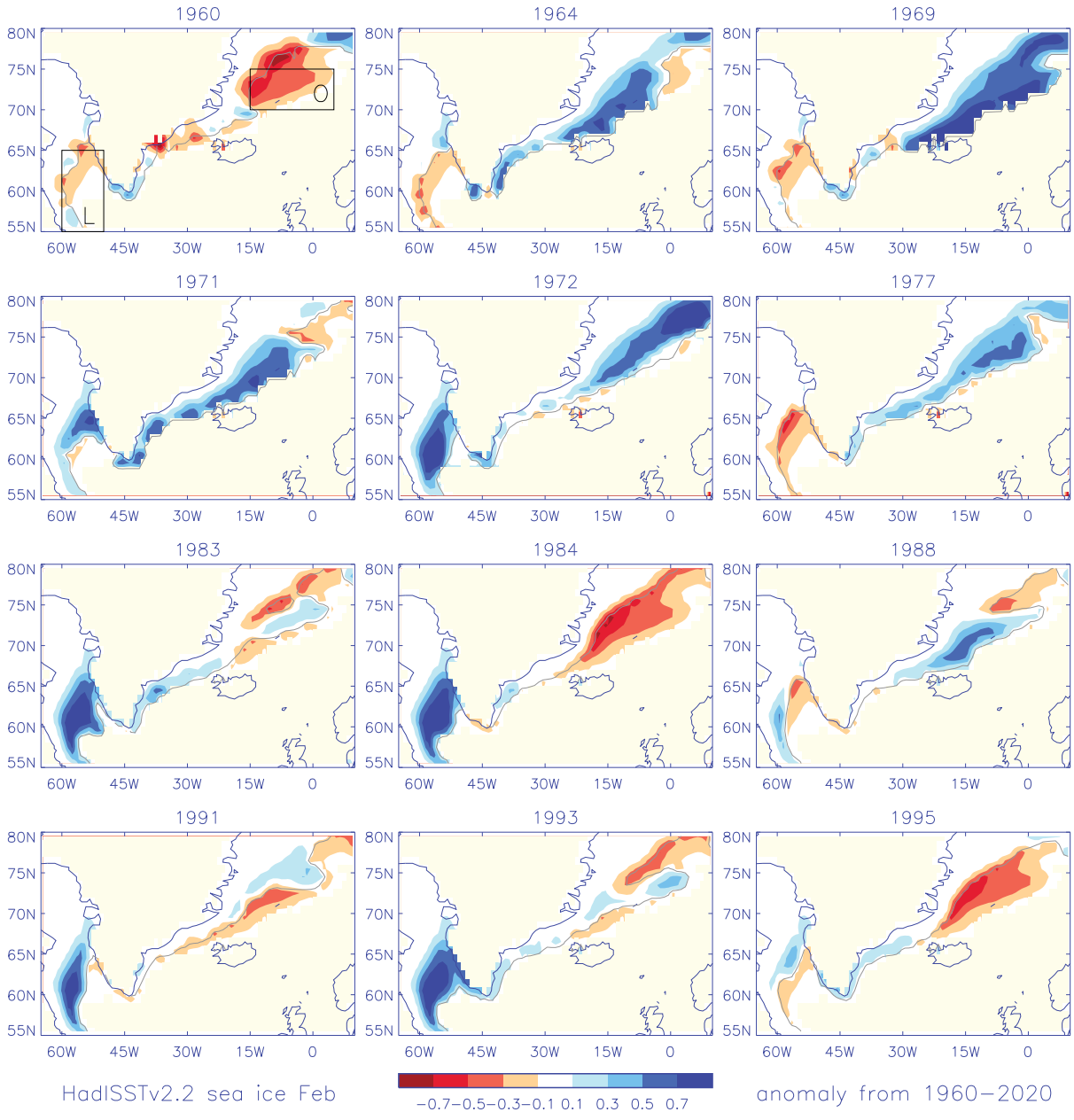
1960
1964
1969
1971
1972
1977
1983
1984
1988
1991
1993
1995
80N
75N
70N
65N
60N
55N
60W
45W
30W
15W
0
L
O
HadISSTv2.2 sea ice Feb
−0.7 −0.5 −0.3 −0.1 0.1 0.3 0.5 0.7
anomaly from 1960−2020

Figure 3.

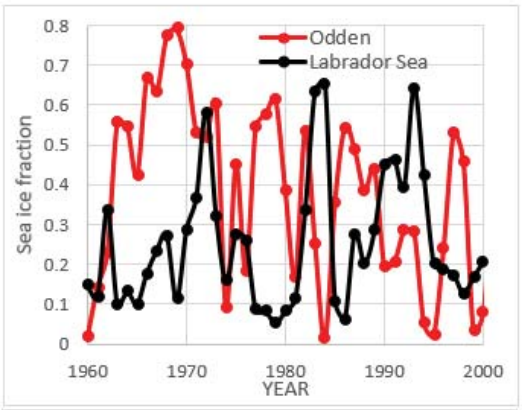
Odden
Labrador Sea
Sea ice fraction
YEAR

(a)

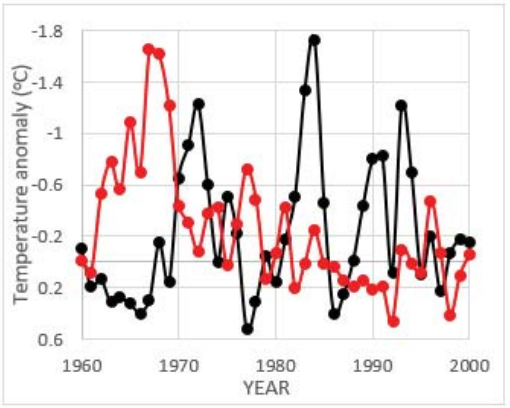
Temperature anomaly (ºC)
YEAR

(b)

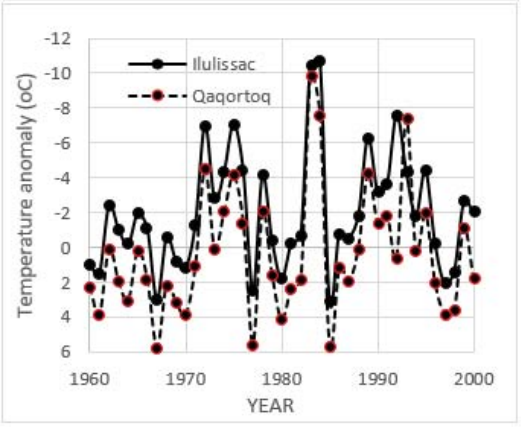
Ilulissac
Qaqortoq
Temperature anomaly (oC)
YEAR

(c)

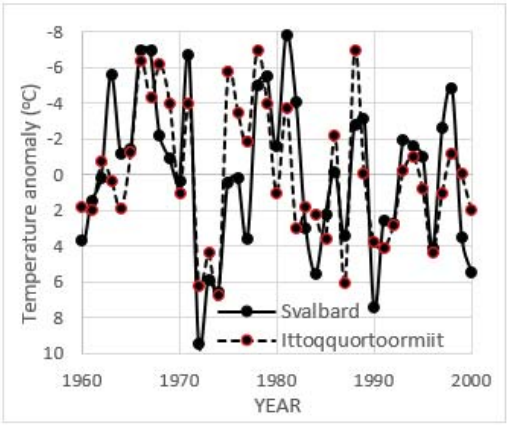
Svalbard
Ittoqquortoormiit
Temperature anomaly (ºC)
YEAR

(d)

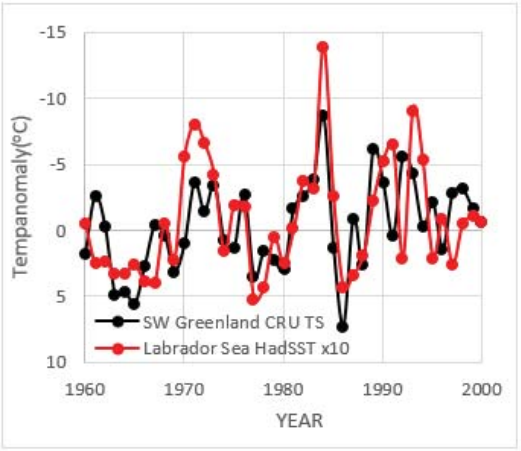
SW Greenland CRU TS
Labrador Sea HadSST x10
Tempanomaly(ºC)
YEAR

(e)

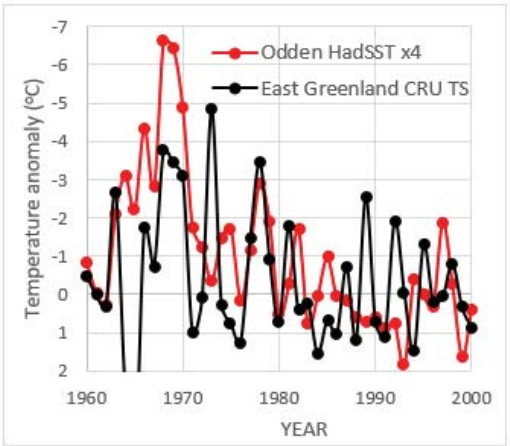
Odden HadSST x4
East Greenland CRU TS
Temperature anomaly (ºC)
YEAR

(f)

Figure 4.

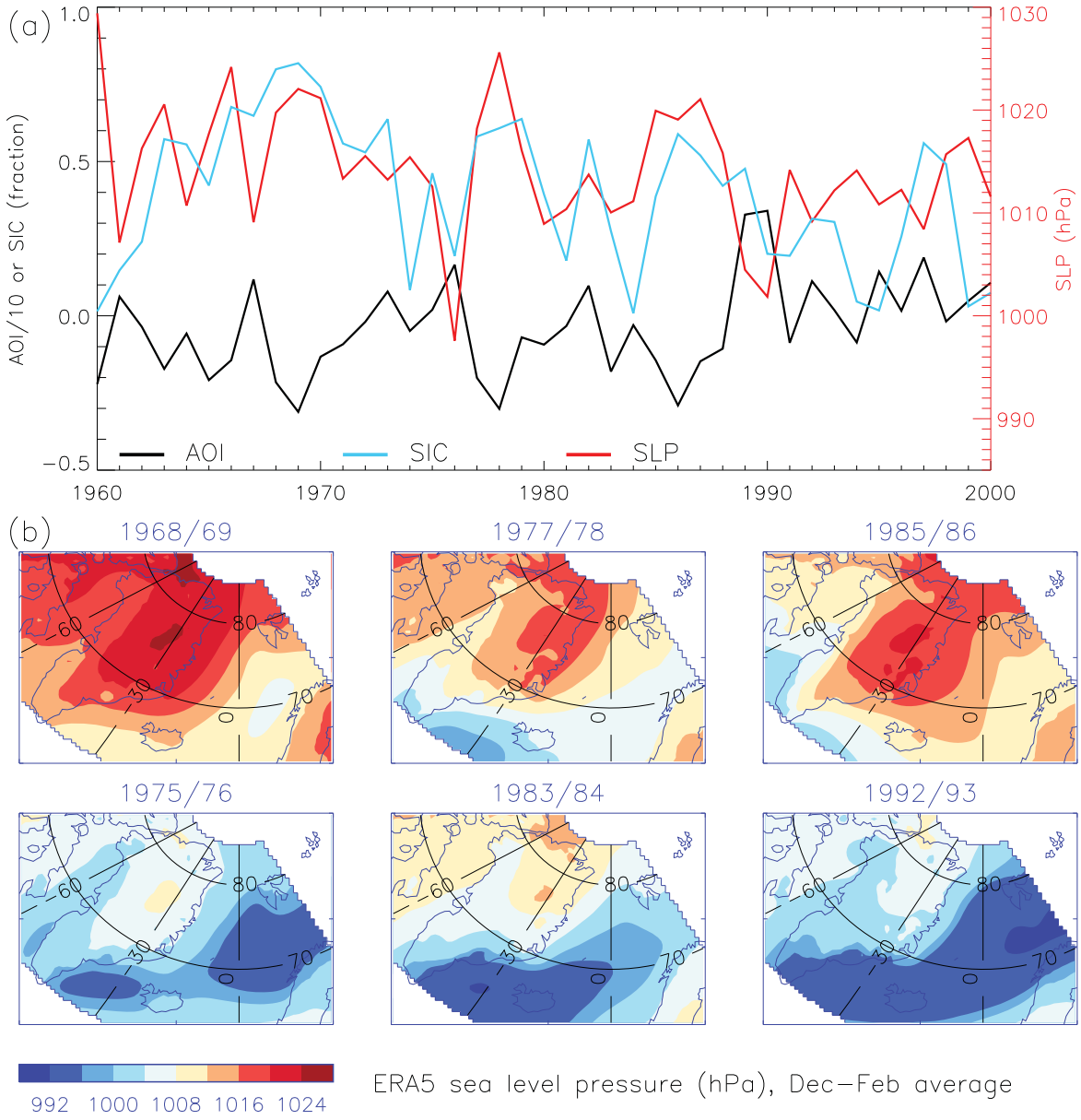
(a)
1.0
0.5
0.0
−0.5
AOI/10 or SIC (fraction)
1030
1020
1010
1000
990
SLP (hPa)
AOI
SIC
SLP
1960
1970
1980
1990
2000
(b)
1968/69
1977/78
1985/86
1975/76
1983/84
1992/93
60
80
30
0
70
992 1000 1008 1016 1024
ERA5 sea level pressure (hPa), Dec–Feb average

Figure 5.

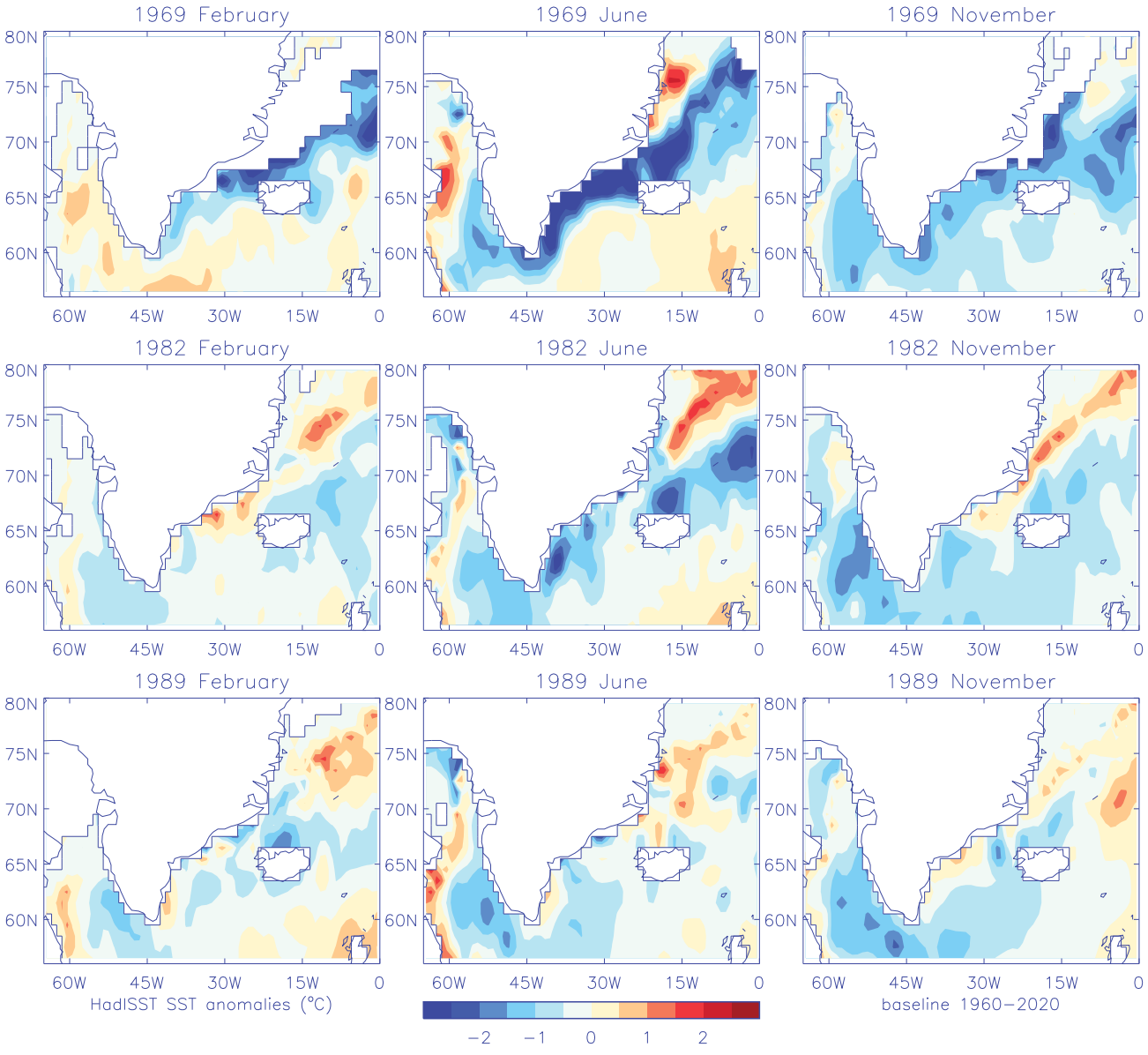
1969 February
1969 June
1969 November
1982 February
1982 June
1982 November
1989 February
1989 June
1989 November
80N
75N
70N
65N
60N
60W
45W
30W
15W
0
HadISST SST anomalies (°C)
−2
−1
0
1
2
baseline 1960–2020

Figure 6.

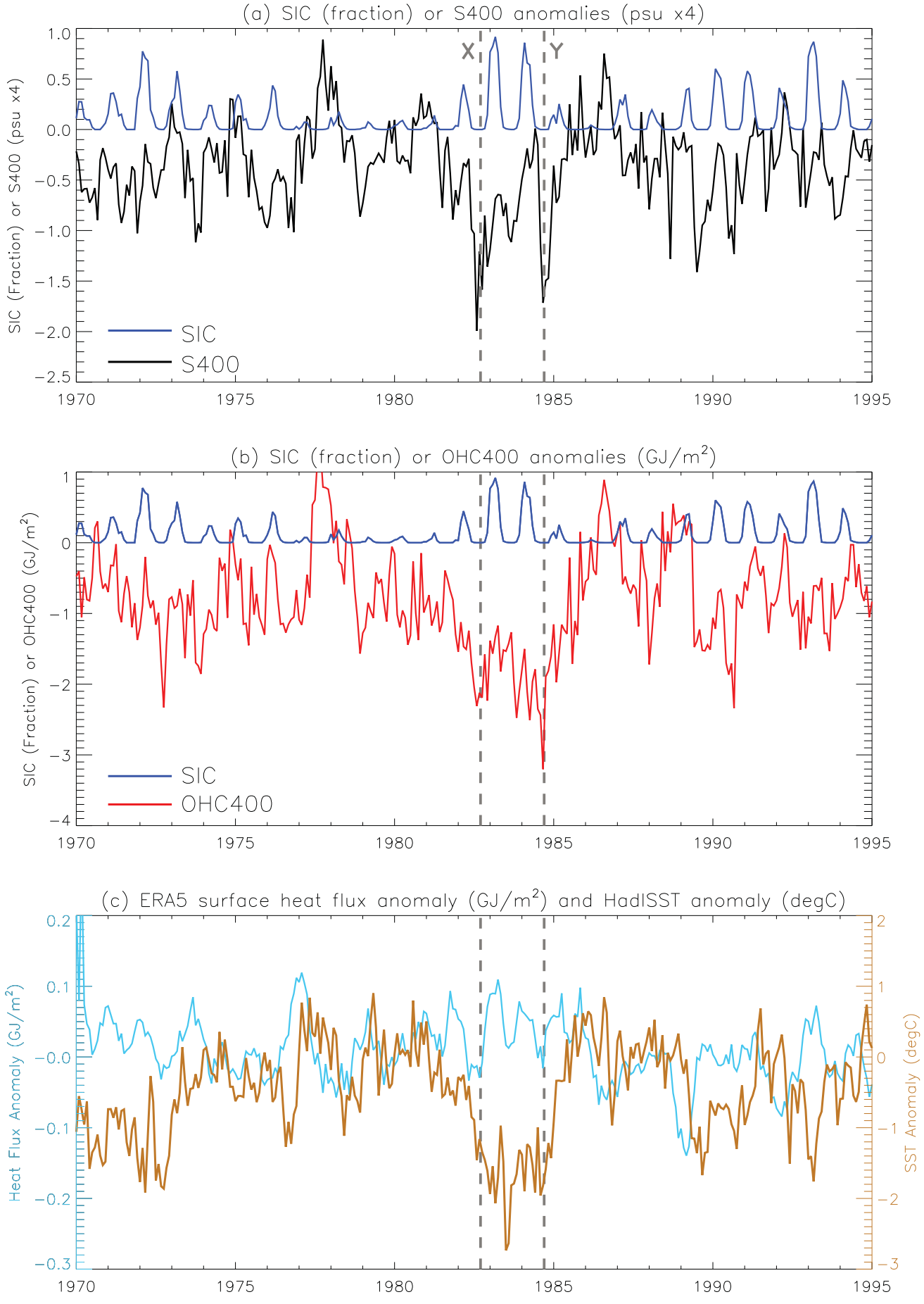
(a) SIC (fraction) or S400 anomalies (psu x4)
SIC (Fraction) or S400 (psu x4)
X
Y
SIC
S400
(b) SIC (fraction) or OHC400 anomalies (GJ/m²)
SIC (Fraction) or OHC400 (GJ/m²)
SIC
OHC400
(c) ERA5 surface heat flux anomaly (GJ/m²) and HadISST anomaly (degC)
Heat Flux Anomaly (GJ/m²)
SST Anomaly (degC)
1970
1975
1980
1985
1990
1995

Figure 7.

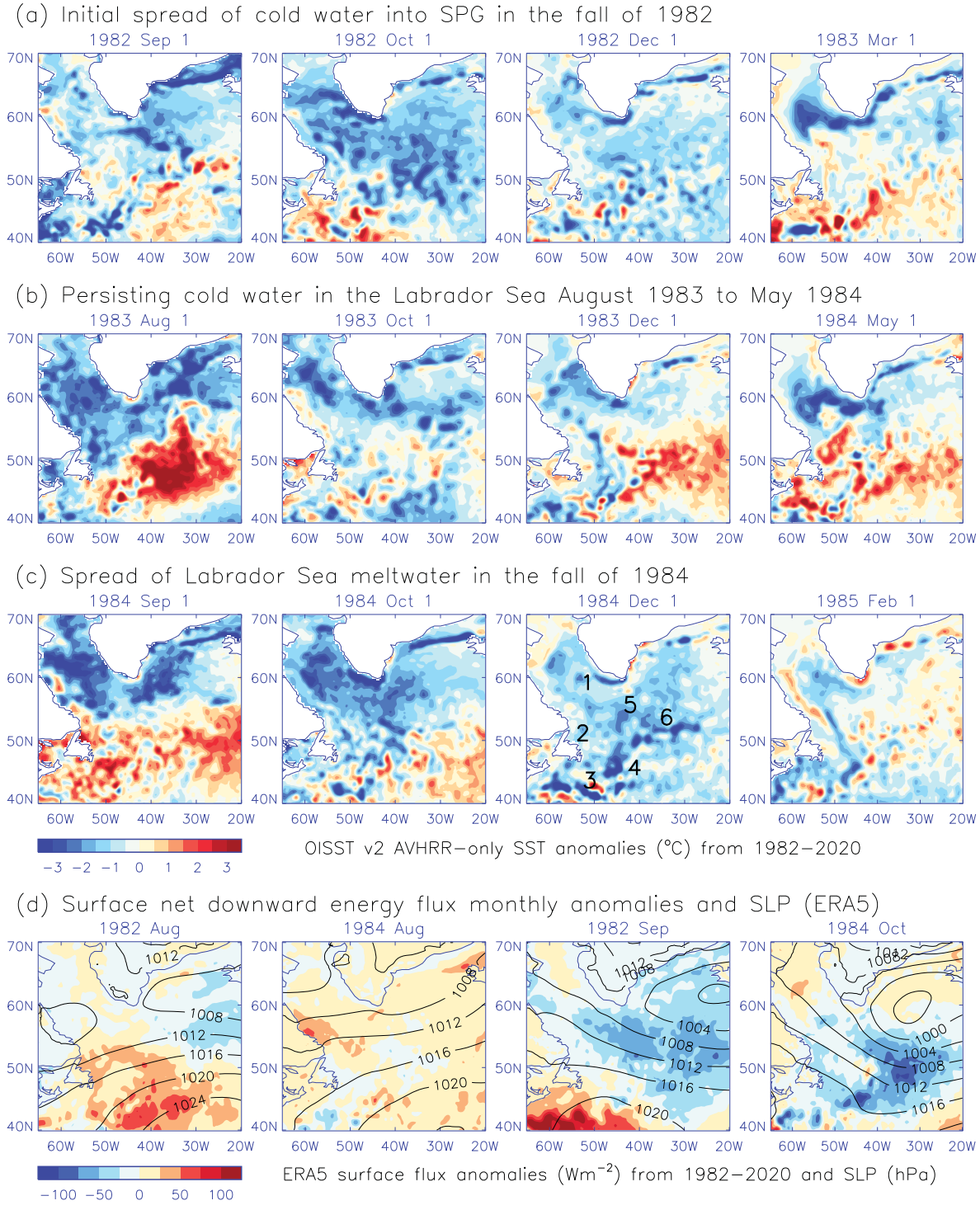
(a) Initial spread of cold water into SPG in the fall of 1982
1982 Sep 1
1982 Oct 1
1982 Dec 1
1983 Mar 1
(b) Persisting cold water in the Labrador Sea August 1983 to May 1984
1983 Aug 1
1983 Oct 1
1983 Dec 1
1984 May 1
(c) Spread of Labrador Sea meltwater in the fall of 1984
1984 Sep 1
1984 Oct 1
1984 Dec 1
1985 Feb 1
1
2
3
4
5
6
70N
60N
50N
40N
60W 50W 40W 30W 20W
−3 −2 −1 0 1 2 3
OISST v2 AVHRR−only SST anomalies (°C) from 1982−2020
(d) Surface net downward energy flux monthly anomalies and SLP (ERA5)
1982 Aug
1984 Aug
1982 Sep
1984 Oct
1004
1008
1012
1016
1020
1024
1000
−100 −50 0 50 100
ERA5 surface flux anomalies (Wm^{-2}) from 1982−2020 and SLP (hPa)